Kinetic Analysis of the Effect of *N*-terminal Acetylation in Thymine DNA Glycosylase

Mary E. Tarantino[1] and Sarah Delaney[2*]

[1]Department of Molecular Biology, Cell Biology, and Biochemistry, Brown University, Providence, RI 02912, United States and [2]Department of Chemistry, Brown University, Providence, RI 02912, United States

ABSTRACT

Thymine DNA glycosylase (TDG) is tasked with initiating DNA base excision repair by recognizing and removing T, U, the chemotherapeutic 5-fluorouracil (5-FU) and many other oxidized and halogenated pyrimidine bases. TDG contains a long, unstructured *N*-terminus that contains four known sites of acetylation: lysine (K) residues 59, 83, 84, and 87. Here, K to glutamine (Q) mutants are used as acetyl-lysine (AcK) analogues to probe the effect of *N*-terminal acetylation on the kinetics of TDG. We find that mimicking acetylation affects neither the maximal single-turnover rate k_{max}, nor the turnover rate k_{TO}, indicating that the steps after initial binding, through chemistry and product release, are not affected. Under sub-saturating conditions, however, acetylation changes the processing of U substrates. Subtle differences among AcK analogues are revealed with 5-FU in single-stranded DNA. We propose that the subtleties observed among the AcK analogues may be amplified on the genomic scale, leading to regulation of TDG activity. *N*-terminal acetylation, though, may also play a structural, rather than kinetic role *in vivo*.

INTRODUCTION

Genomic DNA is under constant onslaught from a vast array of damaging agents from both exogenous and endogenous sources, resulting in lesions that may prove mutagenic, cytotoxic, or transformative for the cell. Hydrolytic deamination of nucleobases, namely deamination of cytosine (C) to uracil (U) or the epigenetic marker 5-methylcytosine (5-mC) to thymine (T), results in a U:guanine (G) or T:G mismatch that, if left unrepaired, results in a C to T transition mutation. [1-3] The base excision repair (BER) pathway is responsible for repairing these and other nucleobase lesions.[4,5] BER is initiated by a glycosylase specific to the nucleobase lesion, which excises the damaged base leaving an abasic (apurinic/apyrimidinic; AP) site. AP endonuclease 1 (APE1) nicks the DNA backbone, allowing for insertion of a C by DNA polymerase β (polβ), and restoration of the strand by DNA ligase.[4,5] There are four human glycosylases that recognize and remove uracil from the genome: uracil DNA glycosylase (UDG/UNG), single strand-selective monofunctional uracil DNA glycosylase (SMUG1), thymine DNA glycosylase (TDG), and methyl binding domain 4 (MBD4). [5,6] Within this group, both TDG and MBD4 also remove T from T:G mispairs, specifically within the 5'-CpG-3' dinucleotide context.[5-16]

TDG is a 46 kDa enzyme with three structural regions: the unstructured *N*-terminus (residues 1-108), the catalytic domain (residues 109-308), and the unstructured *C*-terminus (residues 309-410).[12,13,17-19] NMR studies have demonstrated that the *N*-terminus has a different conformation when TDG is bound to a T substrate versus a U substrate: when bound to T, this region folds back upon the catalytic domain, while when bound to U, this region is extended and in contact with the DNA.[20] In addition to U and T, TDG excises several nucleobases from the genome, including ethenocytosine, oxidized

and halogenated uracil derivatives such as 5-fluorouracil (5-FU), and the oxidized forms of 5-mC 5-formylcytosine (5-fC) and 5-carboxycytosine (5-caC), with specificity for 5'-CpG-3' dinucleotide contexts.[7-11,15,16,21-24] TDG, furthermore, displays differential excisional rates depending on the substrate: those substrates that more readily flip into the active site and have decreased *N*-glycosidic bond stability are excised faster.[10,25] Importantly, TDG exhibits high levels of end-product inhibition regardless of substrate, that is, high affinity for the AP site.[26,27] Its removal of 5-fC and 5-caC ties TDG to active demethylation, which is crucial during epigenetic programming and reprogramming, especially during gametogenesis and embryogenesis.[14,15,21,28,29] Because of this essential epigenetic role, TDG is the only glycosylase known to exhibit embryonic lethality.[28] TDG, additionally, may have roles that are unrelated to its glycosylase activity, as it has been shown to interact with a wide array of other proteins, including transcription factors, chromatin remodelers, proliferating cell nuclear antigen (PCNA), kinases, the acetyltransferase CBP/p300, and the deacetylase SIRT1.[30-40]

TDG not only interacts with kinases and acetyltransferases, but also undergoes post-translational modification (PTM), on both the *N*- and *C*- termini. Lysine (K) 330 in the *C*-terminus serves as a site of SUMOylation.[41-44] This PTM significantly hinders the ability of TDG to perform chemistry,[44] while also decreasing the affinity of TDG for the product AP site while maintaining affinity for the substrate.[41,43] It has been proposed that SUMOylation may enable TDG to serve a chromatin "reader" function, rather than as a glycosylase,[44] or conversely, to allow for turnover of the enzyme.[41,43,45] The *N*-terminus, on the other hand, contains several PTM sites: K59, K83, K84, and K87 are sites of acetylation by CPB/p300, while serine (S) residues 85 and 88 are phosphorylated by

protein kinase C (Figure 1a).[31,36,46] Phosphorylation does not change the Michaelis-Menten constants of TDG, though it is mutually exclusive with acetylation, leading to the hypothesis that the role of phosphorylation is to prevent acetylation of the nearby K.[46] The role of acetylation, however, is less clear. Acetylation has been suggested to decrease the activity of TDG on T and U substrates, while simultaneously to increase the activity on 5-FU substrates.[31] These studies, however, were performed on enzymatically acetylated TDG, and therefore it remains to be determined how acetylation of each K contributes to these observations. Furthermore, CBP/p300 is known to acetylate K in clusters,[33, 47] thereby indicating the possibility that K83, K84, and K87 may be acetylated together.

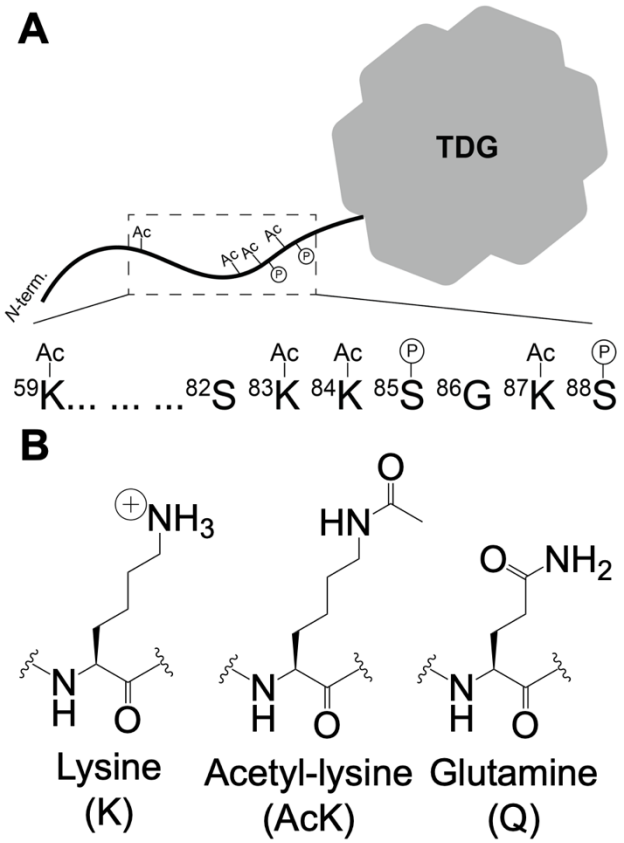

Figure 1. Graphical representation of TDG and structural comparison of amino acids used as analogs in this study. (A) The unstructured *N*-terminus of TDG contains several post-translational modification (PTM) sites:

acetylation (Ac) at lysine (K) residues 59, 83, 84, and 87; and phosphorylation (℗) at serine (S) residues 85 and 88. (B) Structural comparison of K, acetyl-lysine (AcK), and glutamine (Q), the AcK analog used in this study.

TDG is deacetylated by the NAD^+-dependent deacetylase SIRT1, which has been implicated in the cellular and organismal response to caloric restriction, healthspan and lifespan extension, and the response of certain neoplasms to chemotherapeutics.[31,48-53] SIRT1 targets have been identified throughout the BER pathway, including other glycosylases, APE1, and polβ.[54-56] The redox and metabolic states of the cell can determine NAD^+ levels and availability. Metabolism, therefore, directly influences the enzymes, pathways, and processes regulated by SIRT1, including BER.[53,57] Furthermore, knockdown of SIRT1 in several cell lines sensitized the cells to the chemotherapeutic 5-FU. [49,58] The authors suggest that the increased sensitivity is due to the acetylation and therefore increased excisional activity of TDG on 5-FU.[58] In this case, increased excision of 5-FU without subsequent completion of BER leads to an overwhelming DNA damage response (DDR) resulting in cell death.

5-FU is a chemotherapeutic agent often used with other agents in the treatment of many cancers, including colorectal carcinoma and acute myeloid leukemia.[59-63] It was initially designed as an inhibitor of thymidylate synthase (TS) that would disrupt the balance of nucleotides in the dNTP pool and result in a “thymine-less death”, however further mechanisms of action, including those involving BER, contribute to its efficacy.[59,62] Serving as a TS inhibitor, the relative dUTP:dTTP ratio in the dNTP pool increases, resulting in increased incorporation of U into the genome during replication. 5-FU also finds its way into the dNTP pool as 5-FdUTP, and can also be incorporated into the genome during replication.[59,62] A recent study demonstrated that much of U and 5-FU

incorporated during replication is removed at the replication fork by UNG.[64] If, however, the lesions are not removed during replication, such as with UNG inhibition, they persist.[64] The persistent U and 5-FU are subject to repair, including removal by TDG, resulting in AP sites that may be close to one another and on opposite strands. These AP sites may be processed by APE1 or may undergo hydrolysis prior to APE1 processing. The number of strand breaks in this case exceeds the capabilities of polβ and ligase, resulting in single- and double-strand breaks that initiate the DDR. An overwhelming DDR triggers cell death.[59,62]

Given the possible implication of TDG, and specifically acetylated TDG, in the cellular response to 5-FU, we set out to understand how acetylation modulates the kinetics of this enzyme through mutants that mimic acetyl-lysine (AcK; AcK analogues). We have found that neither the maximal single turnover rate (k_{max}) nor the rate of turnover (k_{TO}) of TDG is changed in these analogues, though there is likely a decrease in the affinity for U substrates. Additionally, we have determined that 5-FU in single-stranded DNA is a substrate for TDG, and that this substrate reveals subtle distinctions among the different sites of acetylation in the AcK analogues. The potential biological implications of these findings are discussed.

MATERIALS AND METHODS

Oligonucleotide synthesis and purification

Oligonucleotide sequences are based on those of M. T. Bennett *et al.*[10] and M. T. Morgan *et al.*[11] The sequence of the lesion-containing strand is as follows: 5'-CAC TGC TCA XGT ACA GAG C, in which "X" denotes T, U, or 5-FU. The sequence of its complement is 5'- GCT CTG TAC GTG AGC AGT G, such that the lesion "X" is paired

opposite G in the single CpG dinucleotide of the resulting duplex. Oligonucleotides were synthesized on a MerMade 4 (BioAutomation) using standard phosphoramidite chemistry. All reagents were purchased from Glen Research. The final dimethoxytrityl group was retained for HPLC purification at 90 °C (Agilent PLRP-S column, 250 mm × 4.6 mm; A= 100 mM triethylammonium acetate [TEAA] in 5% [v/v] aqueous acetonitrile [MeCN], B= 100 mM TEAA in MeCN; 5:95 to 30:70 A:B over 30 min at 1 mL/min). Oligonucleotides were subject to detritylation by incubation for 60 min at room temperature in 20% (v/v) aqueous glacial acetic acid. The reaction was quenched by precipitation of the oligonucleotides in room-temperature ethanol. A second HPLC-purification was then performed at 90 °C (Agilent PLRP-S column, 250 mm × 4.6 mm; A= 100 mM triethylammonium acetate [TEAA] in 5% [v/v] aqueous acetonitrile [MeCN], B= 100 mM TEAA in MeCN; 0:100 to 25:75 A:B over 40 min at 1 mL/min). The purified oligonucleotides were flash-frozen with liquid nitrogen, lyophilized, and resuspended in storage buffer (10 mM Tris-HCl pH 8.0, 30 mM NaCl, 1 mM EDTA). The concentration of purified oligonucleotide was determined by absorbance at 260 nm, using extinction coefficients calculated by the OligoAnalyzer 3.1 (Integrated DNA Technologies; https://www.idtdna.com/calc/analyzer).

Site-directed mutagenesis of TDG

The pET-28a plasmid containing wild-type human TDG (pET-28a_TDG-WT) was a generous gift from the laboratory of Alexander C. Drohat (University of Maryland School of Medicine). Site-directed mutagenesis (SDM) was accomplished using the Q5 Site-Directed Mutagenesis Kit (New England BioLabs) with primers (Integrated DNA Technologies) designed by the NEBaseChanger tool (New England BioLabs; http://nebasechanger.neb.com/) (Table S1) following the manufacturer's instructions.

Briefly, Q5 2X Master Mix, forward primer (final concentration 0.5 μM), reverse primer (final concentration 0.5 μM), pET-28a_TDG-WT (29.4 ng), and ddH_2O were mixed in a PCR tube and placed on the thermocycler. The PCR reaction was performed: initial denaturation at 98 °C for 30 s; 25 cycles of denaturation for 10 s at 98 °C, annealing at 58 °C (K83Q; K84Q; 3Q), 59 °C (K87Q), or 62 °C for 30 s, and extension at 72 °C for 195 s; final extension at 72 °C for 2 min. Following PCR, the kinase, ligase, and DpnI (to remove WT plasmid) treatments were performed by mixing the PCR product, 2X KLD Reaction Buffer, 10X KLD enzyme mix, and ddH_2O and incubating at room temperature for 5 min. The mutagenized plasmids were transformed into chemically-competent DH5α *E. coli* (New England BioLabs) by first incubating the preceding reaction with thawed *E. coli* on ice for 30 min. The bacteria were then heat-shocked at 42 °C for 30 s and immediately placed on ice for 5 min. To this mixture room-temperature SOC media (New England BioLabs) was added, and the tube was shaken at 37 °C and 250 rpm for 60 min. The cells were carefully mixed, and were spread on Luria Broth (LB) agar bacterial selection plates containing 50 μg/mL kanamycin sulfate. Plates were incubated overnight at 37 °C.

The following day, eight colonies per mutagenesis were selected and each used to inoculate 5 mL autoclaved LB media containing 50 μg/mL kanamycin sulfate in vented bacterial culture tubes. Tubes were shaken at 225 rpm overnight at 37 °C. Plasmids were extracted from the bacteria using the QIAprep Spin Miniprep Kit (Qiagen) following the manufacturer's protocol. Success of the mutagenesis was confirmed by Sanger sequencing of the mutagenized plasmids by GeneWiz using the universal T7 primer.

Glycosylase expression and purification

Recombinant TDG (WT and mutants) was expressed and purified as previously reported with slight modifications.[13] BL21(DE3) *E. coli* cells (New England BioLabs) were transformed with TDG-containing plasmid (WT or mutants) according to the manufacturer's instructions and spread onto LB agar bacterial selection plates containing 50 μg/mL kanamycin sulfate. A single colony was chosen to inoculate 5 mL LB media with 50 μg/mL kanamycin sulfate in a vented bacterial culture tube. This tube was shaken at 225 rpm overnight at 37 °C. The following morning, the full 5 mL were used to inoculate 100 mL LB with 50 μg/mL kanamycin sulfate which was then shaken at 37 °C and 180-200 rpm until OD_{600}=0.6-0.8. At this time, the 100 mL of growing *E. coli* were used to inoculate two 1 L LB with 50 μg/mL kanamycin each (50 mL of *E. coli* into each flask). The mixtures were shaken at 180 rpm, 37 °C until OD_{600}=0.6-0.8. At this time, the temperature was lowered to 15 °C and the cultures shook for 30 min at 180 rpm. Expression was then induced with isopropyl β-D-1-thiogalactopyranoside (IPTG) to a final concentration of 0.4 mM and allowed to continue for 16 h. Bacteria were pelleted by centrifugation at 5,000 × g for 15 min at 4 °C, flash-frozen in liquid nitrogen, and stored at -80 °C until lysis.

The bacterial pellets were thawed on ice, followed by resuspension in 25 mL lysis buffer (50 mM NaP_i pH 8.0, 10 mM imidazole, 300 mM NaCl, 10 mM β-mercaptoethanol [βME]) containing complete protease inhibitor tablet (1 tablet per 25 mL; Millipore Sigma). The cell suspension was stirred on ice at 4 °C for 20 min to homogenize the suspension, flash-frozen in liquid-nitrogen, and stored at -80 °C until purification.

The cell suspension was thawed in a room-temperature bath for approximately 30 min and was transferred to ice to finish thawing. To the thawed cell suspension, powdered

lysozyme (Fisher Scientific) was added to a final concentration of 1 mg/mL and gently stirred on ice in the cold room for 20 min. At this time, benzonase nuclease (Millipore Sigma) was added and the mixture stirred for 30 min (until the viscosity was similar to water). The lysate was cleared by centrifugation at 23,000 ×g for 30 min at 4 °C and syringe-filtered through a 0.22 μM poly-ethylene sulfonate (PES) membrane in preparation for purification.

All following purification steps were performed by fast protein liquid chromatography on an ÄKTA FPLC (Amersham Biosciences). The filtered lysate was first loaded by syringe onto a HiTrap His 5 mL nickel affinity column (Cytiva) equilibrated with lysis buffer (50 mM NaP_i pH 8.0, 10 mM imidazole, 300 mM NaCl, 10 mM β-mercaptoethanol [βME]). The column was washed with 50 mL High Salt Ni^{2+} Buffer (50 mM NaP_i pH 8, 10 mM imidazole, 1M NaCl, 10 mM β-ME) followed by 50 mL Low Salt Ni^{2+} Buffer (50 mM NaP_i pH 8, 20 mM imidazole, 300 mM NaCl, 10 mM β-ME). TDG was eluted from the nickel column with the following gradient: A=Low Salt Ni^{2+} Buffer, B=Ni^{2+} Elution Buffer (50 mM NaP_i pH 8, 500 mM imidazole, 300 mM NaCl, 10 mM β-ME); 100:0 to 0:100 A:B over 100 mL at 5 mL/min. A final 25 mL wash of 100% Ni^{2+} Elution Buffer at 5 mL/min ensured elution of all TDG. Fractions containing TDG, as determined by absorbance at 280 nm and SDS-PAGE, were combined for further ion-exchange purification.

In preparation for anion exchange, TDG-containing fractions were dialyzed against Exchange Buffer A (EB-A; 20 mM HEPES pH 7.0, 75 mM NaCl, 1 mM dithiothreitol [DTT], 0.2 mM ethylene diamine tetraacetic acid [EDTA]) using 6K MWCO cellulose dialysis tubing (Fisher Scientific) for 90 min, with a buffer change at 60 min. Dialyzed TDG was

syringe-filtered through 0.22 μm PES membrane and loaded by syringe onto a 5 mL HiTrap Q Anion Exchange Column (Cytiva) equilibrated with EB-A. The column was then washed with 50 mL EB-A. TDG was eluted from the anion exchange column with the following gradient: 100:0 to 0:100 EB-A: Elution Buffer B (EB-B; EB-A + 1 M NaCl) over 100 mL at 5 mL/min. Fractions containing TDG, as determined by absorbance at 280 nm and SDS-PAGE, were combined and the salt concentration in the buffer dropped to <100 mM NaCl by the addition of Salt Drop Buffer (EB-A+10 mM NaCl). The TDG-containing solution was then syringe-filtered through a 0.22 μm PES membrane and loaded by syringe onto a HiTrap SP Cation Exchange Column (Cytiva). The column was washed with 50 mL EB-A, and TDG was eluted from the column with the following gradient: 100:0 to 0:100 EB-A: Elution Buffer B (EB-B; EB-A + 1 M NaCl) over 90 mL at 3 mL/min. Fractions containing TDG as determined by absorbance at 280 nm were analyzed by SDS-PAGE. Only those fractions with >95% purity determined by staining were combined. Combined TDG fractions were dialyzed against 2X Storage Buffer (40 mM HEPES pH 7.5, 200 mM NaCl, 2 mM DTT, 1 mM EDTA) overnight at 4 °C using 5K MWCO dialysis tubing. The following morning, fresh 2X Storage Buffer was added and TDG dialyzed for 3 h.

Dialyzed TDG was concentrated using a Vivaspin™ 5K MWCO centrifugal concentrator (Sartorius) at 4,000 rpm at 4 °C until the final volume was <1 mL. A small volume of the TDG was reserved for analysis by ESI mass spectrometry, and to the remainder an equal volume of glycerol was added to generate 1X Storage Buffer (20 mM HEPES pH 7.5, 100 mM NaCl, 1 mM DTT, 0.5 mM EDTA, 50% [v/v] glycerol). TDG in 1X Storage Buffer was aliquoted into 10 μL single-use fractions, flash-frozen with liquid

nitrogen, and stored at -80 °C until use. Concentration was determined by the Bradford assay using bovine γ-globulin standards.

Glycosylase kinetics experiments

Samples of DNA substrate and glycosylase were prepared. The lesion-containing strand carrying a T, U, or 5-FU was 5'-^{32}P end-labeled using T4 polynucleotide kinase (New England BioLabs) following the manufacturer's protocol. For duplex substrates, radiolabeled lesion strand was annealed to its complement (1:1.5 molar ratio) in ANL Buffer (10 mM Tris-HCl, pH 8.0, 30 mM NaCl) by heating to 95 °C for 4 min and cooling at a rate of 1 °C/min to 25 °C. For ss5-FU substrates, radiolabeled lesion strand was subjected to the same annealing conditions as duplex substrates in ANL Buffer. For single-turnover kinetic experiments, 50 nM-2 μM substrate solutions and 500 nM-4 μM TDG solutions were prepared separately in Buffer TNK (20 mM Tris-HCl (pH 7.6), 25 mM NaCl, 75 mM KCl, 1 mM EDTA, 1 mM DTT, 10 μg/mL BSA). For multiple-turnover kinetic experiments, 0.5-4 μM substrate solutions and 20-600 nM TDG solutions were prepared separately in Buffer TNK. All solutions were pre-incubated at 37 °C for 2 min prior to initiating time courses. For experiments with T and U duplex substrates and ss5-FU, enzyme and substrate solutions were mixed and quenched by hand. At time t=0, equal volumes of DNA substrate and TDG were mixed for final concentrations of 25 nM-1 μM DNA and 250 nM-2 μM TDG (single-turnover) or 0.25-2 μM DNA and 10-300 nM TDG (multiple-turnover) and incubated at 37 °C. At the designated time points, a small volume of the reaction solution was removed and quenched with equal volume 1 M NaOH (final concentration 500 mM NaOH). This method was used for two replicates each of T and U duplex substrates under STO and MTO conditions with TDG^{WT}, TDG^{K83Q}, TDG^{K84Q}, and

TDG^{K87Q}. Alternatively, equal volumes of DNA substrate and TDG were mixed for individual time points, incubated at 37 °C, and quenched with 1 M NaOH (final concentration 500 mM NaOH). This method was used for all other reactions under STO and MTO conditions with T and U duplex substrates, and ss5-FU. The time points for T duplex substrates for both STO and MTO conditions were the following (min): 0.167, 0.5, 1, 2, 3, 5, 10, 15, 30, 45, 60. The time points for U duplex substrates for both STO and MTO were the following (min): 0.167, 0.333, 0.5, 0.75, 1, 1.5, 2, 3, 5, 7.5, 10, 15, 20, 30 (and 45, 60 for 25 nM U under STO conditions only). The time points for ss5-FU substrates under STO and MTO conditions were the following (min): 0.5, 1, 2, 3, 5, 7.5, 10, 15, 20, 30, 45, 60.

For each time course, three negative controls were included. The no treatment (NT) sample was prepared by incubating DNA at room temperature for the duration of the reaction; this sample was not quenched with NaOH. The no enzyme (-E) sample was prepared by mixing equal volume of DNA substrate and Buffer TNK, incubating at 37 °C for the longest time point, and adding 1 M NaOH quench (final concentration 500 mM NaOH). The quench control (QC) was prepared by mixing DNA substrate and 1 M NaOH (double the volume of DNA), followed by immediate addition of TDG (equal volume to DNA) and incubation at 37 °C for the longest time point. For experiments with 5-FU:G, DNA substrate and TDG were mixed at 37 °C and quenched with 1 M NaOH in a Rapid Quench Flow apparatus (RQF-3; KinTek Corp.). The -E sample was prepared by mixing DNA substrate and Buffer TNK in the RQF for the longest time point followed by quench with 1 M NaOH. The time points under STO conditions were the following (s): 0.005, 0.01,

0.025, 0.05, 0.1, 0.25, 0.5, 0.75, 1, 1.5, 2, 3, 5. The time points under MTO conditions were the following (s): 0.025, 0.05, 0.1, 0.25, 0.5, 0.75, 1, 1.5, 2, 3, 5, 7.5, 10, 12, 15.

Following completion of the time course, all samples (except NT) were heated to 90 °C for 2 min to induce strand breaks at abasic sites. DNA substrate and product were resolved by 12% denaturing PAGE, imaged by phosphorimagery, and quantitated by densitometry.

The fraction product, F_p, at each time point t, was determined as follows:

$$F_p(t) = \frac{\delta_p(t)}{\delta_s(t) + \delta_p(t)}$$

in which $\delta_s(t)$ and $\delta_p(t)$ represent the densities of substrate and product bands, respectively, at time t. The product yield at each time point, $P(t)$, was corrected for baseline levels of damage as follows:

$$P(t) = \frac{F_p(t) - F_p(0)}{1 - F_p(0)}$$

in which $F_p(0)$ is the fraction product in the QC sample for manually-quenched experiments, or the fraction product in the –E sample for the RQF-quenched experiments. For STO experiments, the product yield for each time course was plotted as a function of time and fit using nonlinear least-squares regression to the modified first-order integrated rate law:

$$P(t) = P(\infty)(1 - e^{-k_{obs}t})$$

where $P(t)$ is the product yield at time t, $P(\infty)$ is the maximum product yield, and k_{obs} is the observed rate of product formation (Kaleidagraph). For MTO experiments, the product yield for each time course was plotted as a function of time and fit using nonlinear least-squares regression to burst plus linear function:

$$P(t) = A(1 - e^{-k_{obs}t}) + vt$$

where *P(t)* is the product yield at time *t, A* is the amplitude of the burst, k_{obs} is the observed rate of the burst, and *v* is the steady-state rate of the reaction (Kaleidagraph). The overall rate of the reaction k_{TO} is calculated by dividing *v* by the concentration of enzyme, [E], in the reaction. The time courses depicted for k_{TO} are single representative time courses at the same concentration of enzyme over a wide range of enzyme concentrations measured. The reported rates represent mean ± standard error. Individual *A* and *v* values for the MTO time courses are given in Table S2.

Extrapolation of k_{max} and K_D for ss5-FU substrates

To extrapolate k_{max} and K_D values for TDG^{WT} and AcK analogues, manual time courses under STO conditions were performed as described above with the following final concentrations: 25 nM or 250 nM DNA, 1 μM TDG; and 500 nM or 1 μM DNA, and 2 μM TDG. The individual k_{STO} rates were determined by fitting the fraction product by nonlinear least-squares regression to a modified first-order integrated rate law as described above. The rates were then plotted as a function of potential [ES] and fit to a hyperbolic curve by nonlinear least-squares regression (Kaleidagraph):

$$k_{STO} = \frac{k_{max}[ES]}{K_D + [ES]}$$

where k_{STO} is the observed STO rate, k_{max} the extrapolated maximal STO rate, [ES] the potential [ES] concentration, and K_D the extrapolated binding constant.[12]

Statistical Analysis

Values for k_{max} and k_{TO}, and were compared individually within each substrate by analysis of variance (ANOVA) followed by a *post hoc* Tukey test for pairwise comparison (α=0.01) using R.[65] Here we consider p<0.01 to be significant.

RESULTS AND DISCUSSION

Rationale

To examine the effect of acetylation on K residues in the *N*-terminus of wild-type TDG (TDG^{WT}), we chose to mutate K to Q (Figure 1b). Q is similar both in size and charge to AcK, and has been experimentally validated as a suitable analogue.[66,67] Each AcK site was mutated individually to Q. Given the propensity of CBP/p300 to acetylate K near AcK,[33,47] we also mutated the cluster of three lysine residues (K83, K84, K87) to Q, which here will be called 3Q (Table 1). Collectively, we refer to these K to Q mutants as TDG-AcK analogues.

TDG	Sequence
WT	*N*- …^{59}K…^{82}SKKSGKS…-*C*
K59Q	*N*- …^{59}Q…^{82}SKKSGKS…-*C*
K83Q	*N*- …^{59}K… ^{82}SQKSGKS…-*C*
K84Q	*N*- …^{59}K …^{82}SKQSGKS…-*C*
K87Q	*N*- …^{59}K… ^{82}SKKSGQS…-*C*
3Q (K83Q-K84Q-K87Q)	*N*- …^{59}K… ^{82}SQQSGQS…-*C*

Table 1. List of TDG AcK analogs and corresponding amino acid sequence used in this study.

We chose to use a previously published 19mer oligonucleotide sequence[10,11] that contains a centrally located CpG site and allows for binding of only a single TDG molecule (Figure 2a). It is important to note that the substrates examined in this study—T, U, and 5-FU—are in the 5′-XpG/CpG-3′ sequence context (in which X is a lesion). TDG contains residues responsible for recognizing the 5′-CpG-3′ on the complement strand, and prefers substrates in this sequence context.[12,13]

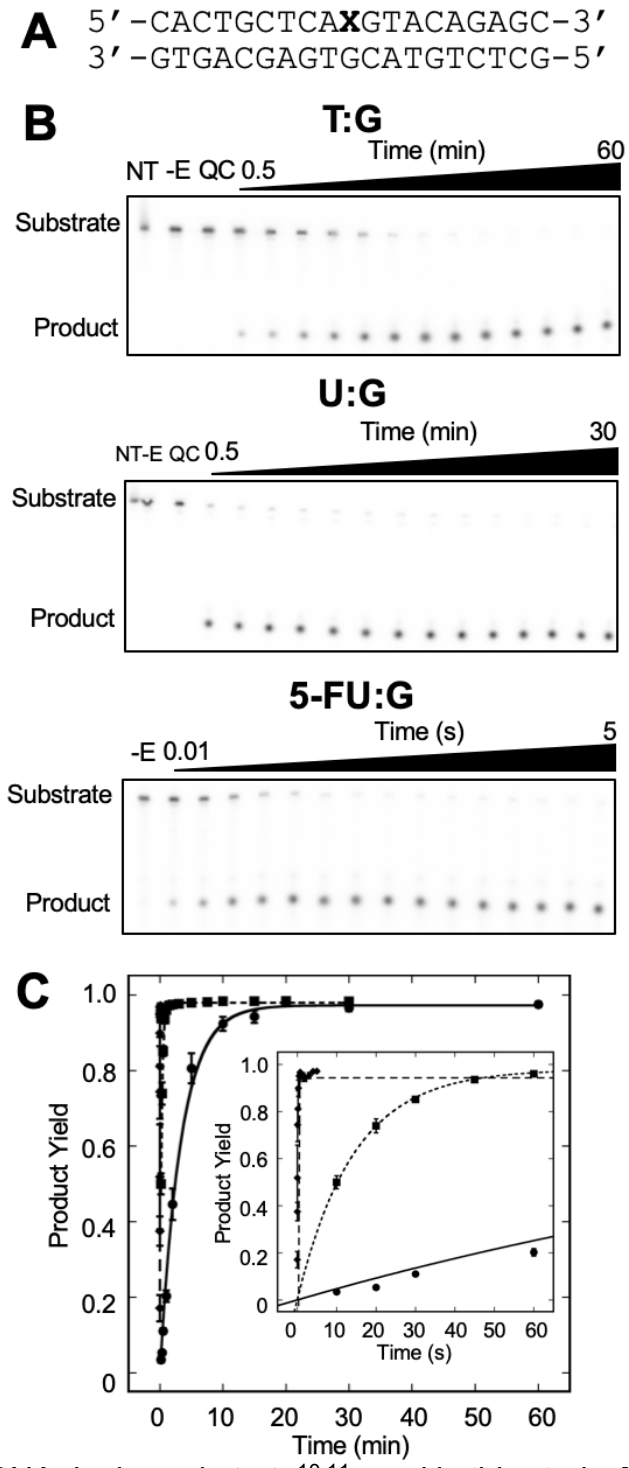

Figure 2. (A) DNA duplex substrate[10,11] used in this study. **X** represents T, U, or 5-FU, positioned in a 5'-XpG/CpG-3' sequence context. (B) Representative denaturing PAGE depicting the excision of T, U, or 5-FU from duplex substrates by TDG^{WT} under STO conditions. NT, no treatment; -E, no enzyme; QC, quench control. (C) Corresponding graphs depicting the excision of T (circles), U (squares), or 5-FU (diamonds) from duplex

substrate by TDG^{WT}. Data were fit to a single exponential equation and error bars represent standard error.

We probed the effects of *N*-terminal acetylation on TDG using two broad sets of conditions: single turnover (STO) conditions, in which [TDG]>>[DNA], and multiple turnover (MTO) conditions, in which [DNA]>>[TDG]. In the minimal kinetic scheme of TDG (Scheme 1), TDG first binds to the DNA substrate. The lesion X— either T, U, or 5-FU— is flipped into the active site, the equilibrium of which is described as K_{flip}. The *N*-glycosidic bond is cleaved ($k_{chemistry}$; k_{chem}), generating an AP site. The product is then released. It is important to note that TDG has significant affinity for abasic sites,[26,68] and the AP-containing DNA may be re-bound by TDG.

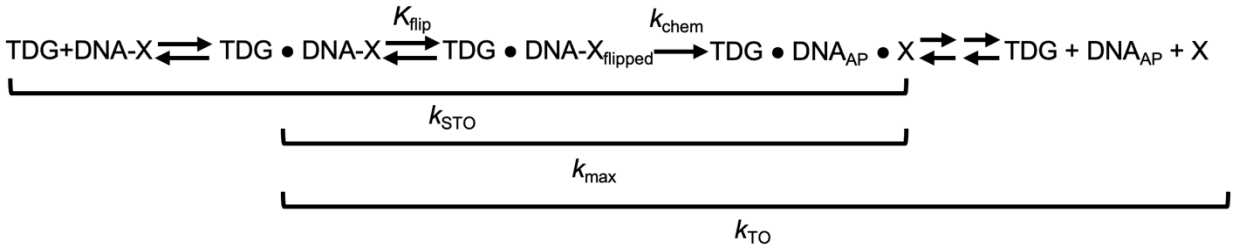

Scheme 1. Minimal kinetic scheme of TDG. TDG first binds to the DNA substrate containing the lesion (X). TDG flips the lesion into the active site, the equilibrium of which is given by K_{flip}. TDG then cleaves the *N*-glycosidic bond (k_{chem}). The free nucleobase and AP-containing DNA products are released. Notably, TDG can re-bind the AP-containing DNA (end-product inhibition). The observed STO rate (k_{STO}) is representative of steps up to and including chemistry. The maximal STO rate (k_{max}) is representative of the steps after initial binding up to and including chemistry. The MTO rate of turnover (k_{TO}) is representative of all steps after initial binding, including any end-product inhibition.

The rates obtained from STO experiments (k_{STO}) give information about the events up to and including the first irreversible step, which for TDG is glycosidic bond cleavage. Under conditions in which [TDG]>[DNA] and [TDG]>>K_D , k_{STO} collapses to the maximal

STO rate (k_{max}), which is reflective of the rates after binding and up to and including chemistry, which can be expressed in as in Eq. 1:[25,69]

$$k_{\max} = k_{\text{chem}} \frac{K_{\text{flip}}}{1+K_{\text{flip}}} \quad (1).$$

MTO experiments give information about the entire catalytic cycle. As is true for many glycosylases and other BER enzymes, the rate-determining step of TDG occurs after chemistry.[12,13,26] This results in biphasic product accumulation (also called burst kinetics) prior to attainment of the steady-state phase of the reaction (pre-steady state).[27,70] The burst represents the first turnover of the enzyme, with the subsequent linear phase indicative of subsequent turnovers and is equivalent to the initial velocity (v_0). Under conditions in which [DNA]>>K_m, v_0 collapses to k_{TO}[E], where k_{TO} represents the rate of turnover of the enzyme. Given the high affinity of TDG for the AP-containing DNA product,[26,68] we cannot assume that k_{TO} is equivalent to k_{cat}, which assumes no end-product inhibition of the enzyme.[71] In performing experiments under both STO and MTO conditions, we gain insight into the full catalytic cycle of TDG in both the acetylated and non-acetylated states.

k_{max} is not affected in the *N*-terminal AcK analogues

To evaluate the kinetic steps up to and including chemistry, we performed time courses under STO conditions. To ensure [TDG]>>K_D for determination of k_{max}, experiments were performed with at least two different enzyme and substrate concentrations. As expected, TDG^{WT} exhibits monophasic kinetics and converts all substrates fully to product over the course of the reaction, though at much different time scales (Figure 2b, c). This significant difference in the rates of excision is reflected in the k_{max} values: TDG-WT excises T with k_{max}=0.30 $\pm$ 0.3 min^{-1} and U and 5-FU ~14 and

~3,300 times faster, respectively (Table 2), similar to previously reported rates.[10,11,13,25,26,44,72] The increased rates of excision have been attributed both to increased base flipping[25] and increased rate of chemistry due to decreased *N*-glycosidic bond stability[10] for U and 5-FU relative to T.

Enzyme	Substrate	k_{max} (min^{-1}) [a]	k_{max} relative to T:G	k_{STO} (min^{-1}) [a,b], yield (%)	k_{TO} (min^{-1}) [a]	k_{TO} relative to T:G	k_{max}/k_{TO}
TDG^{WT}	T:G	0.30 ± 0.03 (4)	1		0.007 ± 0.002 (7)	1	43
	U:G	4.2 ± 0.2 (3)	14	4.1 ± 0.6*, 91 (4)	0.14 ± 0.05 (5)	20	30
	5-FU:G	1000 ± 290 (3)	3300		2.5 ± 1.0 (3)	360	400
TDG^{K59Q}	T:G	0.42 ± 0.01 (7)	1		0.003 ± 0.001 (7)	1	140
	U:G	4.4 ± 0.4 (5)	10	3.6 ± 0.10*, 96 (3)	0.04 ± 0.01 (7)	10	150
	5-FU:G	940 ± 130 (3)	2200		3.4 ± 0.8 (6)	100	280
TDG^{K83Q}	T:G	0.36 ± 0.02 (4)	1		0.002 ± 0.001 (9)	1	180
	U:G	4.4 ± 0.3 (3)	12	1.9 ± 0.2*, 92 (3)	0.09 ± 0.03 (9)	45	50
	5-FU:G	1260 ± 320 (3)	3500		2.2 ± 0.5 (3)	1100	570
TDG^{K84Q}	T:G	0.46 ± 0.05 (4)	1		0.009 ± 0.002 (6)	1	51
	U:G	4.2 ± 0.3 (3)	9.1	3.6 ± 0.5*, 93 (4)	0.03 ± 0.01 (4)	3.3	140
	5-FU:G	980 ± 280 (3)	2100		3.4 ± 0.7 (3)	110	290
TDG^{K87Q}	T:G	0.42 ± 0.05 (4)	1		0.006 ± 0.003 (5)	1	70
	U:G	3.9 ± 0.2 (3)	9.3	2.1 ± 0.3*, 90 (4)	0.11 ± 0.04 (4)	18	35
	5-FU:G	790 ± 14 (3)	1900		2.3 ± 0.4 (3)	380	340
TDG^{3Q}	T:G	0.43 ± 0.05 (4)	1		0.004 ± 0.002 (3)	1	110
	U:G	3.1 ± 0.3 (5)	7.2	2.9 ± 0.2*, 75 (3) 0.04 ± 0.01, 25 (3)	0.05 ± 0.01 (7)	13	62
	5-FU:G	750 ± 130 (3)	1700		4.5 ± 0.9 (4)	1100	170

Table 2. Rates of processing duplex substrates by TDG^{WT} and AcK analogs. [a]Rates are reported as mean ± standard error (n). [b]25 nM U:G substrate, 1000 nM TDG. Asterisk (*) denotes $p<0.01$ versus slow phase of 3Q by ANOVA and post-hoc Tukey test for pairwise comparisons for U:G 25 nM substrate.

All TDG-AcK analogs also exhibit monophasic kinetics for T, U, and 5-FU substrates (Figure 3, Table 2). For the excision of T and U, k_{max} is not statistically different for any of the TDG-AcK analogs compared to TDG^{WT} (Figure 3a, b). Though these values are not statistically different from WT or each other in the context of this short oligonucleotide, it is interesting to consider the slight variation among the TDG-AcK analogs. The k_{max} for TDG^{WT} is 14 times faster for U, while TDG^{K84Q}, TDG^{K87Q}, and TDG^{3Q} are less than 10 times faster (Table 2). The difference in relative k_{max} values suggests a possible shift in the kinetic discrimination of the enzyme between T and U substrates with

acetylation. NMR studies have demonstrated that the *N*-terminal tail of TDG—specifically the region containing the acetylation and phosphorylation sites—exhibits different conformations when bound to a T or U substrate.[20] When bound to T, the *N*-terminal tail folds back upon the catalytic domain and likely contacts acidic residues on the surface of the enzyme, while when bound to U, the tail is extended, and may be in contact with the DNA.[20] Acetylation of the *N*-terminus may change the interaction of the tail with the catalytic domain and/or the adjacent DNA, resulting in the observed discrepancies in relative k_{max}.

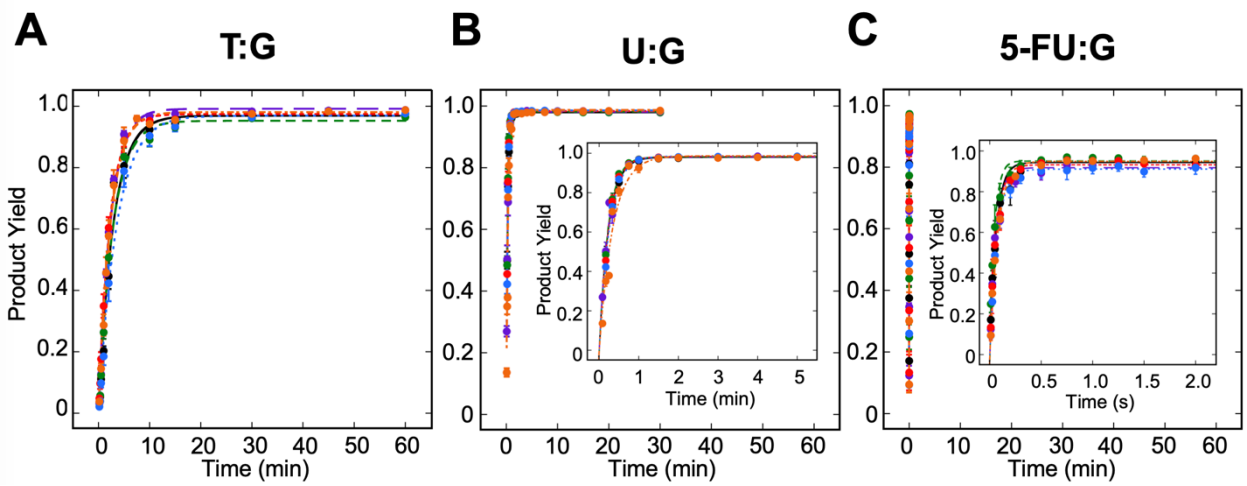

Figure 3. k_{max} is not affected in the TDG-AcK analogues. STO time courses were used to determine the effect of *N*-terminal acetylation of TDG on the excision of T (A), U (B), and 5-FU (C) from duplex substrates. Reactions consisted of 25 nM (T, 5-FU) or 250 nM (U) duplex substrate and 1000 nM TDG in Buffer TNK (20 mM Tris-HCl (pH 7.6), 25 mM NaCl, 75 mM KCl, 1 mM EDTA, 1 mM DTT, 10 μg/mL BSA). Data were fit to a single exponential equation and error bars represent standard error. Black, TDG^{WT}; purple, TDG^{K59Q}; green, TDG^{K83Q}; red, TDG^{K84Q} ; blue, TDG^{K87Q}; orange, TDG^{3Q}.

For every TDG-AcK analogue, the excision of 5-FU is much faster than T and U, with k_{max} values of ~1000 min^{-1} (Figure 3c). Similar to the excision of T and U, the k_{max} values are not significantly different from each other on this substrate.

Taken together, these data indicate that acetylation of the *N*-terminus of TDG does not affect k_{max} on short oligonucleotides.

STO kinetics are changed in acetylation analogues at lower U substrate concentrations

In determining k_{max}, we performed experiments at varying enzyme and substrate concentrations to ensure measurement of the maximal single turnover rate. Though we did not observe differences among these titrations for T and 5-FU, there was a striking difference between TDG^{3Q} and all other TDG-AcK analogs in the excision of U (Figure 4). In contrast to TDG^{WT} and all other analogs at the substrate concentrations examined, TDG^{3Q} exhibits biphasic kinetics. The fast phase, comprising 75% of the product accumulation, proceeds at a rate $k_{STO\text{-}fast}=2.9 \pm 0.2$ min^{-1}, which is not statistically different from k_{STO} for the other TDG-AcK analogs under these conditions nor from k_{max} for U excision by any TDG-AcK analog. The slow phase, however, which accounts for 25% of the product, occurs at a rate of $k_{STO\text{-}slow}=0.04 \pm 0.01$ min^{-1}. This rate is significantly different from both the $k_{STO\text{-}fast}$ for TDG^{3Q}, k_{STO} under these conditions for all other TDG-AcK analogs, and every k_{max} for excision of U, indicating the measurement of a substrate-dependent rate-determining step prior to chemistry.

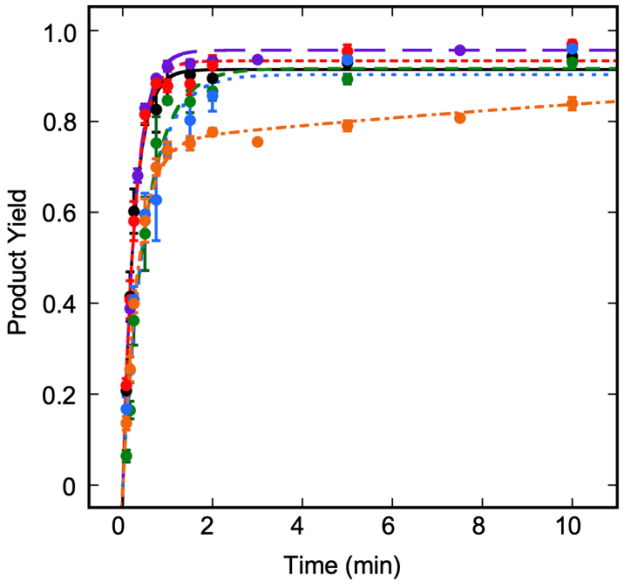

Figure 4. TDG^{3Q} exhibits biphasic kinetics under STO conditions at lower [U]. Reactions consisted of 25 nM U duplex substrate and 1000 nM TDG in Buffer TNK (20 mM Tris-HCl (pH 7.6), 25 mM NaCl, 75 mM KCl, 1 mM EDTA, 1 mM DTT, 10 μg/mL BSA). Data were fit to a single or double exponential equation and error bars represent standard error. Black, TDG^{WT}; purple, TDG^{K59Q}; green, TDG^{K83Q}; red, TDG^{K84Q}; blue, TDG^{K87Q}; orange, TDG^{3Q}.

Furthermore, it is worthwhile to note that, except for TDG^{WT}, the k_{STO} values at 25 nM are generally slower than at 250 nM (Table 2). These results indicate that the pre-chemistry complex (TDG•DNA-$X_{flipped}$, Scheme 1) is not entirely saturated at 25 nM U:G substrate. The single TDG-AcK analogs still display monophasic product accumulation kinetics, however, suggesting the impact of a substrate-dependent step within a single progress curve only when the tail is acetylated. Taken with the slight disparities in relative k_{max} values for T and U excision observed for TDG^{K84Q}, TDG^{K87Q}, and TDG^{3Q}, these data point to a shift in kinetic discrimination of T and U with acetylation.

k_{TO} is not affected in *N*-terminal AcK analogues

To evaluate all steps of the reaction after initial binding, we conducted kinetic time courses under MTO conditions. For all substrates, TDG^{WT} and every TDG-AcK analog

exhibit burst kinetics, in which the first turnover of the enzyme is represented in the exponential rise of the curve, followed by a linear phase reflective of subsequent turnovers (Figure 5). As described above, the biphasic nature of pre-steady state product accumulation indicates the presence of a rate-determining step following chemistry. For the excision of T, k_{TO} is incredibly slow, with k_{TO}<0.01 min^{-1} for TDG^{WT} and the TDG-AcK analogs (Figure 5a, Table 2). This rate translates to k_{TO}<15 day^{-1}. The k_{TO} rates on the short oligonucleotides are not statistically different from each other.

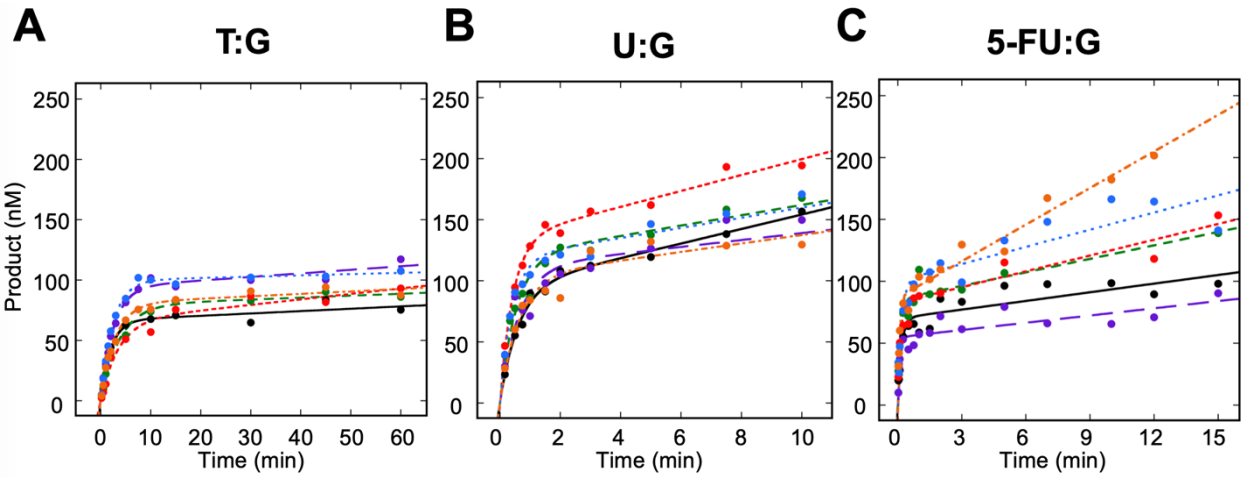

Figure 5. k_{TO} is not affected in the TDG-AcK analogues. Representative MTO time courses depict the effect of *N*-terminal acetylation of TDG on the excision of T (A), U (B), and 5-FU (C) from duplex substrates. Reactions consisted of 1000 nM duplex substrate and 100 nM TDG in Buffer TNK (20 mM Tris-HCl (pH 7.6), 25 mM NaCl, 75 mM KCl, 1 mM EDTA, 1 mM DTT, 10 μg/mL BSA). Data were fit to a biphasic exponential plus linear equation. Black, TDG^{WT}; purple, TDG^{K59Q}; green, TDG^{K83Q}; red, TDG^{K84Q}; blue, TDG^{K87Q}; orange, TDG^{3Q}.

Similar to what was observed under STO conditions, TDG processes and subsequently turns over faster on U and 5-FU compared to T substrates (Figure 5b,c). Indeed, TDG^{WT} has a k_{TO} ~20 and ~350-fold greater for U and 5-FU, respectively, relative to T. Notably, k_{TO} for 5-FU is within the same order of magnitude as k_{max} for U. As

observed for T substrates, for U and 5-FU there is not a statistical difference for the k_{TO} values of TDG^{WT} and the TDG-AcK analogs.

TDG^{K84Q}, however, stands out as having a k_{TO} for U that is less than 5-fold greater than k_{TO} for T, and TDG^{3Q} has relative k_{TO} ~10, again suggesting a possible change from TDG^{WT} in T and U kinetic discrimination. On the other hand, TDG^{K83Q} displays the greatest difference of ~50 between U and T k_{TO}, indicating a potential change from TDG^{WT}, but clearly differently from TDG^{K84Q}.

Furthermore, slight differences among TDG^{WT} and the TDG-AcK analogs are revealed by the k_{max}/k_{TO} values. For TDG^{WT}, k_{max}/k_{TO} are 43, 30, and 400 for T, U, and 5-FU, respectively. TDG^{K87Q} is the only TDG-AcK analogue for which k_{max}/k_{TO} are similar to TDG^{WT} for every substrate. TDG^{K59Q}, on the other hand, is the only analogue with k_{max}/k_{TO} over 100 for both T and U. These ratios would indicate that TDG^{K87Q} is most similar to TDG^{WT} in processing these three substrates, while TDG^{K59Q} is the least similar.

Importantly, there are striking differences in k_{TO} values for T, U, and 5-FU excision for all analogs. As discussed above, k_{TO} is reflective of the slowest step(s) of the reaction, which for TDG occurs after chemistry. In considering the minimal kinetic scheme, these steps encompass nucleobase release, AP site release, and any rebinding of TDG to the AP site (end-product inhibition). Molecular dynamics simulations have suggested that nucleobase release occurs on the nano- to microsecond time scale immediately following chemistry while the AP site is still bound by the enzyme.[73,74] In this case, it is unlikely that nucleobase release is rate-limiting, and thus step(s) beginning with AP-bound TDG contribute to k_{TO}. One may assume, therefore, that the steps governing AP site release and/or rebinding to the AP site would be the same regardless of starting substrate since

the enzyme has reached the same step. Under these assumptions, k_{TO} would be comparable regardless of the substrate. As demonstrated previously[26,27,68] and above, these assumptions do not hold. In this case, there may be more steps to release of an AP site from a T substrate than U, which in turn has more steps than release from a 5-FU substrate. Such step(s) could include, for example, unfurling of the *N*-terminal tail from the catalytic domain in the release of an AP site from T, a step that would not be required in the release of the AP site from U. Under this interpretation, the lower limit for AP site release by TDG is revealed by 5-FU k_{TO} ~2-5 min^{-1}.

5-FU in single-stranded DNA is a substrate for TDG

Experimental evidence indicates that duplex substrates are required for the excision of T and U by TDG.[9,17,21,68] This observation is supported by co-crystal structures of TDG bound to DNA where residues specifically recognize the complementary strand.[12,13] Given how readily not only TDG^{WT}, but also all the TDG-AcK analogs, both excise and turn over 5-FU in duplex DNA, we asked whether 5-FU in single-stranded DNA (ss5-FU) is a substrate for TDG. To test this potentially novel capability of TDG, we incubated ss5-FU with TDG^{WT} and the TDG-AcK analogs. The 5-FU duplex substrate used in the experiments described above served as the positive control. Much to our surprise, we observed excision of 5-FU from the single-stranded substrate by TDG^{WT} and all the TDG-AcK analogs (Figure 6).

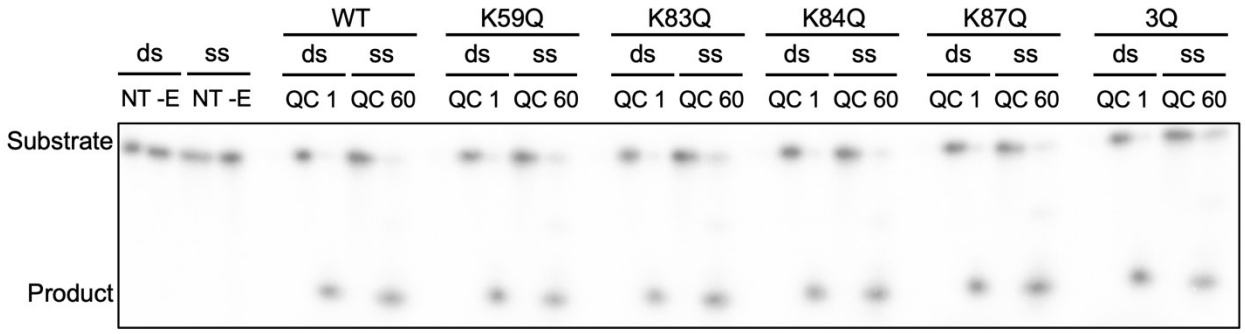

Figure 6. 5-FU in ssDNA is a substrate for TDG. Denaturing PAGE depicting reactions consisting of 25 nM 5-FU duplex (ds) or 250 nM ssDNA (ss) substrate incubated with 1000 nM TDG for 1 min (1) or 60 min (60) in Buffer TNK (20 mM Tris-HCl (pH 7.6), 25 mM NaCl, 75 mM KCl, 1 mM EDTA, 1 mM DTT, 10 μg/mL BSA). NT, no treatment; -E, no enzyme; QC, quench control.

We next endeavored to measure the k_{max} values for excision of ss5-FU, starting with STO conditions that were suitable for the measurement of k_{max} on duplex substrates. To confirm that the rates determined correspond to k_{max}, we performed additional STO experiments at increasing enzyme and substrate concentrations (Figure 7, Figure S3).

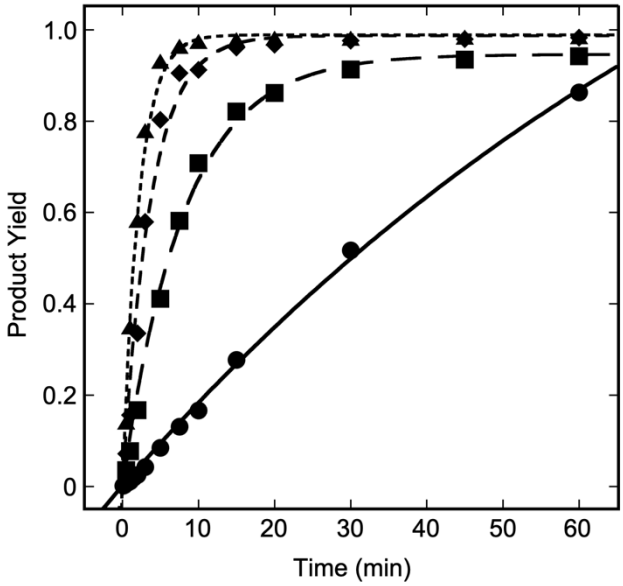

Figure 7. Excision of 5-FU from ssDNA by TDG^{WT} under STO conditions. Reactions were performed with 25 nM DNA, 1000 nM TDG^{WT} (circles), 250 nM DNA, 1000 nM TDG^{WT} (squares), 500 nM DNA, 2000 nM TDG^{WT} (diamonds), and 1000 nM DNA, 2000 nM TDG^{WT} (triangles) in Buffer TNK (20 mM Tris-HCl (pH 7.6), 25 mM NaCl, 75 mM KCl, 1 mM EDTA, 1 mM DTT, 10 μg/mL BSA). Data were fit to a single exponential curve.

When k_{STO} does not increase with increasing [DNA] and [TDG], one knows k_{max} has been reached. At even the highest concentrations tested, which were limited by the concentration of TDG, we could not confirm attainment of k_{max}. Such titrations under STO conditions, however, allow for modeling of both k_{max} and K_D values by fitting the k_{STO} as a function of the potential [ES] concentration:[75]

$$k_{\mathrm{STO}} = \frac{k_{\max}[ES]}{K_{\mathrm{D}}+[ES]} \qquad (2).$$

In modeling of TDG^{WT} (Figure 8), the projected k_{max}=2.3 min^{-1}, which is within an order of magnitude of k_{max} for U excision from duplex and is comparable to k_{TO} for 5-FU on duplex.

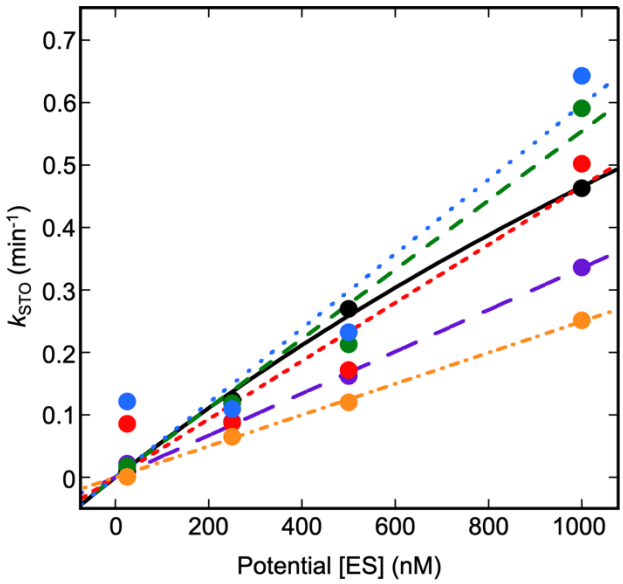

Figure 8. Extrapolation of k_{max} and K_D values from STO experiments with ss5-FU. The observed single turnover rate (k_{STO}) is plotted as a function of potential [ES] and data were fit to a hyperbolic curve. Black, TDG^{WT}; purple, TDG^{K59Q}; green, TDG^{K83Q}; red, TDG^{K84Q}; blue, TDG^{K87Q}; orange, TDG^{3Q}.

Furthermore, the predicted K_D for TDG^{WT} is 4 μM, which is over two orders of magnitude greater than previously measured values for T in duplex substrates (18 nM)[13,76] and over four orders of magnitude greater than K_D values for U in duplex substrates (0.6 nM)[12,76]. Though the k_{max} and K_D values for the TDG-AcK analogs are not as well defined as for TDG^{WT}, comparison of the curves to TDG^{WT} allows for generalizations of relative k_{max} and K_D values (Figure 8). Namely, the TDG^{K59Q} and TDG^{3Q} curves track below TDG^{WT}, suggesting that for these two TDG-AcK analogs, k_{max} may be lower, K_D may be higher, or a combination of the two. On the other hand, the curves of the single AcK analogs in the cluster—TDG^{K83Q}, TDG^{K84Q}, and TDG^{K87Q}—track with or

above WT, indicating that k_{max} may be comparable to or higher than TDG^{WT}, and K_D may be comparable to or lower than TDG^{WT}. Though ss5-FU reveals differences among TDG^{WT} and the TDG-AcK analogs that were less apparent on the duplex substrates, it is important to note that 5-FU is excised from single-stranded DNA at rates orders of magnitude slower than from duplex.

The rate-determining step of ss5-FU processing occurs prior to or at chemistry

Since the modeled k_{max} of ~2 min^{-1} for TDG^{WT} on ss5-FU is comparable to k_{TO} on 5-FU duplex substrates, we asked whether product release is rate-limiting for ss5-FU. If product release is rate limiting, a burst would be observed under pre-steady state MTO conditions, as we observed for T, U, and 5-FU in duplex (Figure 5). On the other hand, if product release is not rate limiting, the burst will be severely depressed or lost, and pre-steady state product will accumulate in a linear manner. We captured the full reaction curve, which demonstrates that the single-site TDG-AcK analogs process ss5-FU faster than TDG^{WT} under these conditions, while TDG^{3Q} processes ss5-FU similarly to TDG^{WT} (Figure 9). By zooming in to the pre-steady state portion of the curve (Figure 9, inset), no burst is observed for any of the TDG enzymes. Therefore, in processing ss5-FU, the rate-determining step of the reaction has shifted from product release to a step before or at chemistry.

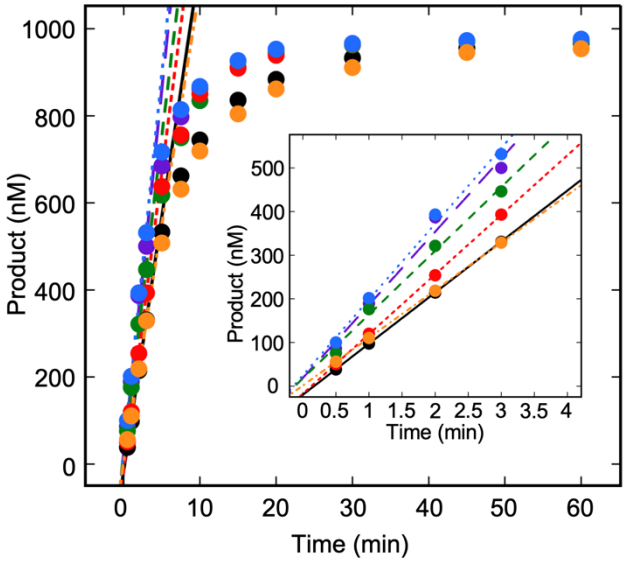

Figure 9. The RDS in the processing of ss5-FU occurs before or at chemistry. Reactions were carried out with 1000 nM ss5-FU and 250 nM TDG in Buffer TNK (20 mM Tris-HCl (pH 7.6), 25 mM NaCl, 75 mM KCl, 1 mM EDTA, 1 mM DTT, 10 μg/mL BSA). The first 3 min of the reaction were fit to a linear equation. Black, TDG^{WT}; purple, TDG^{K59Q}; green, TDG^{K83Q}; red, TDG^{K84Q}; blue, TDG^{K87Q}; orange, TDG^{3Q}.

Biological Implications

Potential implications of TDG acetylation at the molecular level

Here we have demonstrated that AcK analogues in the *N*-terminus of TDG affect neither k_{max} nor k_{TO} on short oligonucleotide substrates for processing T, U, and 5-FU. However, ss5-FU and decreased [U] substrates have revealed subtle differences among TDG^{WT} and the TDG-AcK analogues. Furthermore, mimicking acetylation seems to cause a shift in kinetic discrimination between T and U, namely decreased processing of T relative to the unacetylated state, in accordance with a previous study by Madabushi *et al*.[31] Our results indicate that this shift is the consequence of decreased turnover (k_{TO}) relative to base-flipping and chemistry (k_{max}), which may be from decreased rates of AP site release and/or increased affinity for the free AP site. In a cellular context, this characteristic would translate to increased protection of the highly labile AP site[4,26,27] until processing by APE1.

In addition to decreased processing of T by AcTDG compared to the acetylated state, Madabushi and colleagues also found that AcTDG increased activity on 5-FU substrates.[31] Though our kinetic data with 5-FU in duplex DNA do not reveal differences among TDG^{WT} and the AcK analogs, experimental procedures may account for the seeming disparate results. The TDG used in the investigation by Madabushi *et al*. was enzymatically acetylated by p300 and AcCoA, which could lead to a potentially heterogeneous population of acetylation sites in the *N*-terminus. Furthermore, the concentrations of both duplex DNA and TDG were much lower than those in our reactions. It is worthy of note, however, that we did observe subtle differences among TDG^{WT} and the AcK analogues on the ss5-FU substrate. The much lower concentrations of the experiments by Madabushi *et al*. may be revealing the same subtleties we observe with ss5-FU. That is, only conditions that "challenge" TDG with sub-saturating concentrations of substrate or sub-optimal substrate uncover the effect of *N*-terminal acetylation.

In considering the TDG-AcK analogues, TDG^{K87Q} stands out as processing substrates most similarly to TDG^{WT}, while TDG^{K59Q} is the single AcK analogue that is least similar to TDG^{WT}. Interestingly, comparable conclusions regarding the role of acetylation sites were drawn regarding the glycosylase NEIL2.[77] NEIL2, which is also a target of CBP/p300, has a similar acetylation pattern in its *N*-terminus to TDG: a more *N*-terminal site (K49), and a cluster of three residues closer to the catalytic domain (K149, K150, K153).[77] It was reported that while both K49 and K153 were the main targets for acetylation, decreased activity was observed only when K49 was acetylated, and thus the acetylation of K153 may play a different biological role.[77] NEIL2 K49 is analogous to TDG K59. Mimicking acetylation of TDG K59, as discussed above, leads to activity that is least

similar to TDG^{WT}, suggesting that single acetylation sites outside of clusters may function as a "switch" for changes in activity. TDG K87, the mutation of which leads to the least change in activity from TDG^{WT}, is analogous to NEIL2 K153. TDG K87, and NEIL2 K153, for that matter, may therefore function as "sentinel" acetylation sites, *i.e.* this K is the first to undergo acetylation in the cluster of three. The acetylation of K87 in TDG would serve as the anchor for the bromodomain of CPB/p300, which would then acetylate K83 and/or K84. In this case, the cluster of three K residues serve as tunable activity for TDG, culminating in the acetylation of all three K residues. As demonstrated above, TDG^{3Q} clearly processes U differently than the other TDG-AcK analogues and TDG^{WT}. The acetylation of TDG at K59 versus at the cluster of three may therefore be differentially regulated and serve distinct purposes *in vivo*.

Considering regulation of and roles for TDG acetylation at the cellular level

It is interesting to consider when TDG may undergo acetylation within the cellular context. Studies on other BER enzymes have demonstrated increased acetylation when CBP/p300 is activated.[33,47,54,55,89] These circumstances include cellular stress (*e.g.* oxidative stress and hyperosmolarity), in response to hormones and certain growth factors, and at times of acetyl-coenzyme A (AcCoA) abundance (Figure 10a).[33,47,78,79] In the case of cellular stress, transcription of genes responsible for responding to the stress increases.[66,79,90] Acetylation of TDG and decreased processing of T substrates may therefore be a way to maintain heterochromatin and preserve cellular resources while the cell is trying to maintain homeostasis. It would follow that regulation of TDG in this way may be through acetylation of K59, which would allow for the "switch" in activity necessary for the cell.

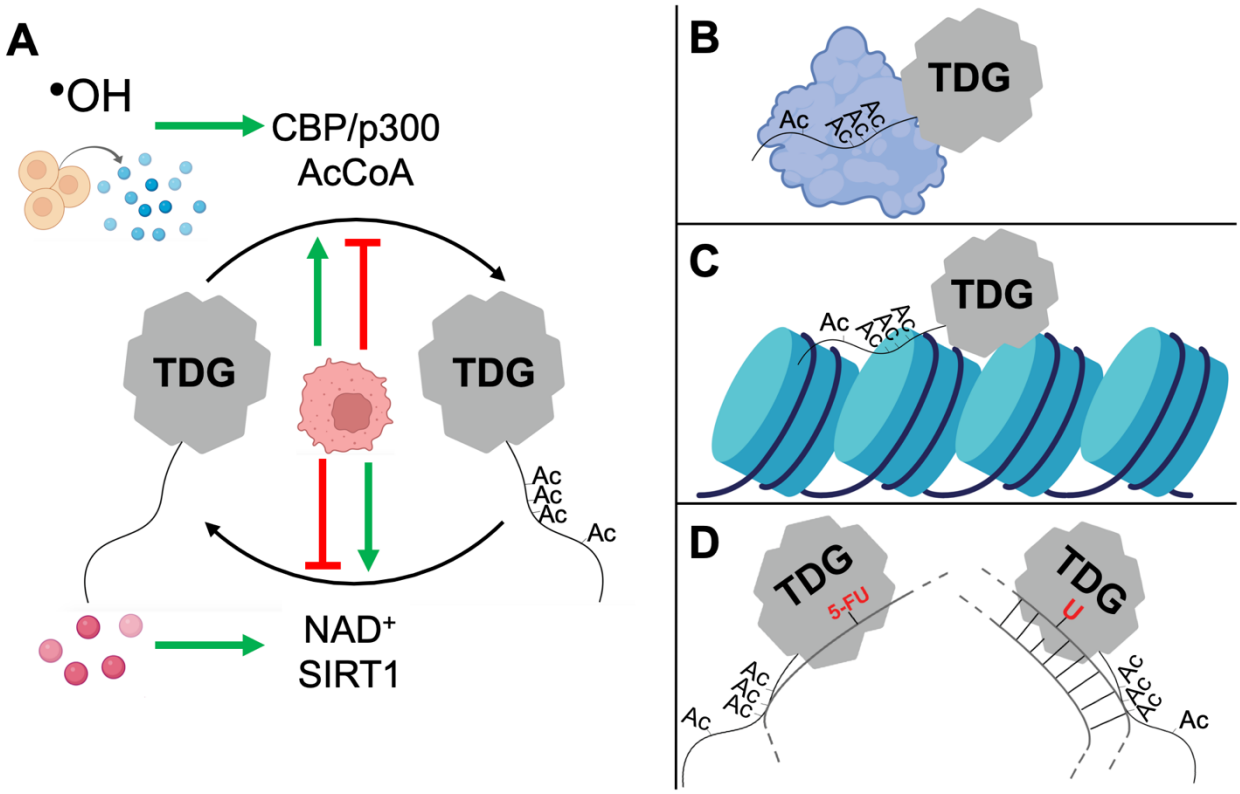

Figure 10. Potential roles and regulation of TDG acetylation within the cell. (A) TDG undergoes acetylation by CBP/p300, which requires the cofactor AcCoA. Cellular stress, including oxidative stress by hydroxyl radicals (·OH), and cellular growth and signaling factors can induce the activity of CBP/p300,[33,47,78,79] leading potentially to greater acetylation of TDG. The NAD^+-dependent SIRT1 deacetylates TDG, which is under the control of small molecules, nutrient availability, and NAD^+/NADH levels.[31,51,80] CBP/p300 and/or SIRT1 can be dysregulated in cancer.[48,49,81-83] (B) Acetylation of the *N*-terminus may promote interactions between TDG and its many protein binding partners.[30-40] (C) Acetylation of the N-terminus may promote LLPS of TDG into the heterochromatic compartment.[84-88] This allows for TDG to access substrates in heterochromatin. (D) The acetylation of the N-terminus leads to differential processing of U duplex and ss5-FU substrates under sub-saturating conditions.

Furthermore, SIRT1 and/or CBP/p300 are found to be under/overexpressed and/or dysregulated in a variety of cancers (Figure 10a).[48,49,81-83] These states would lead to loss of regulation of acetylation of both chromatin and associated enzymes, such as TDG. This could result in an increase of "missed repair" opportunities by TDG. Indeed,

one of the most common mutations found in cancers is the C to T transition mutation, especially in 5′-CpG-3′ dinucleotide contexts.[1-3,49,91] On the other hand, the primary role of acetylation may not be kinetic, but rather structural. As mentioned above, TDG interacts with a multitude of proteins,[30-40] and PTM may promote and/or prevent the association of TDG with certain binding partners (Figure 10b).

The *N*-terminus of TDG shares many features with intrinsically disordered proteins/regions (IDP/Rs):[84, 85] its amino acid composition is rich in glycine (G), S, Q, and tyrosine (Y); it contains several PTM sites, including clustered phosphoserine and AcK sites;[31,36,46] and it is unstructured via NMR.[20] One major characteristic of IDP/Rs is the ability to undergo liquid-liquid phase separation (LLPS); that is, to create a distinct compartment within a liquid mixture, such as oil droplets in water or the nucleolus inside the nucleus.[84,85] For many IDP/Rs, K acetylation promotes phase separation, while serine phosphorylation prevents phase separation.[84,85] Interestingly, previous work has demonstrated that phosphorylation and acetylation of the *N*-terminus of TDG are mutually exclusive, and the authors suggest the primary purpose of phosphorylation is the inhibition of acetylation.[46]

Heterochromatin is known to exist in a phase-separated state inside the nucleus.[84,86,87] Acetylation of TDG, therefore, may promote the separation of the enzyme into the heterochromatic phase, where it can access its substrates (Figure 10c). The Sczepanski laboratory demonstrated the ability of TDG to reversibly condense chromatin, suggesting the enzyme, even in the absence of PTM, is capable of phase separation.[88] Acetylation and phosphorylation of TDG may regulate the phase separation properties of TDG, thereby determining the genomic compartment in which it is active.

This property may be especially important in the removal of the chemotherapeutic 5-FU from the genome (Figure 10d). As demonstrated above, 5-FU in duplex is excised and turned over by TDG at rates orders of magnitude greater than T and U. This brings into question whether the rate of AP site release on which the cell typically relies for regulation of TDG-initiated BER is lost. In the event of incomplete or slower repair by Polβ and ligase, multiple strand breaks proximal to each other could initiate the double-strand break response. If this response overwhelms the cell, it will die by apoptosis (if the machinery is intact), or necrosis. As such, it has been suggested that TDG is the primary glycosylase responsible for cellular sensitivity or resistance to 5-FU.[88,92] A recent study, however, identified UNG in particular, and not TDG, as a modulator of sensitivity to 5-FU incorporated into DNA in a wide variety of colon cancer cell lines.[64] These compelling results suggest that, if TDG does have a role in the cellular response to 5-FU, its role is much more complex than previously appreciated. Even in the case that TDG plays a minor role in the sensitivity of a tumor to 5-FU, our results indicate that, if 5-FU nucleobases persist until discovery by TDG, the enzyme will remove and turnover 5-FU duplex substrates significantly faster than T and U. The typical regulation of TDG as the cell uses for T and U are lost, as TDG is "distracted" by 5-FU over its native substrates.

It is therefore important to consider whether ss5-FU is a relevant substrate for TDG *in cellulo*. We have demonstrated that TDG is capable of excising ss5-FU, though at rates orders of magnitude slower than 5-FU in duplex, indicating that the cellular substrate of 5-FU for TDG is duplex DNA. Ss5-FU does demonstrate, however, that there are subtle differences among TDG^{WT} and the TDG-AcK analogues. Though these differences are likely insignificant on short oligonucleotide substrates, they would be amplified on the

genomic scale. That is, discrepancies in rates that are insignificant on a short oligonucleotide may prove significant inside the cell. As such, amplification of minute differences may translate to fine-tuned regulation of TDG enzymatic activity so that key epigenetic information is maintained or (purposefully) lost by the cell.

Conclusions

In this study, we have demonstrated that acetylation analogues in the *N*-terminus of TDG exhibit changes neither in k_{max} nor in k_{TO} on short oligonucleotides, as well as the novel capability of TDG to excise 5-FU from ssDNA. Furthermore, the processing of ss5-FU by TDG exhibits different kinetics than the duplex substrates, with the rate-determining step occurring prior to or at chemistry. Subtle differences among the AcK analogues are revealed by ss5-FU, differences that may prove significant when placed on the genomic scale. Furthermore, acetylation of the *N*-terminus of TDG may play regulatory and/or structural roles, with kinetic variation playing a secondary role. These observations augment the argument for the consequential role of TDG in cellular sensitivity and/or resistance to 5-FU in the treatment of cancer.

SUPPORTING INFORMATION

The Supporting Information is available free of charge on the ACS Publications website. DNA sequences used for primers for site-directed mutagenesis, MTO kinetic parameters, and supplementary figures (including gel images and kinetic graphs).

AUTHOR INFORMATION

Corresponding Author

Sarah Delaney - *Department of Chemistry, Brown University, Providence, Rhode Island 02912, United States*; orcid.org/0000-0002-8366-3808; Phone: +1 401 863 1000; Email: sarah_delaney@brown.edu

Author

Mary E. Tarantino - *Department of Molecular Biology, Cell Biology, and Biochemistry, Brown University, Providence, Rhode Island 02912, United States*; orcid.org/ 0000-0002-5220-8706.

Funding

This research was supported by National Science Foundation (MCB-2111680). M.E.T was supported by the National Institutes of Health/National Cancer Institute (F30 CA243362).

Notes

The authors declare no competing financial interest.

ACKNOWLEDGMENT

We thank Dr. Alexander C. Drohat (University of Maryland School of Medicine) for the TDG expression plasmid. This research was supported by National Science Foundation (MCB-2111680) and the National Institutes of Health/National Cancer Institute (F30 CA243362; MET). We also thank members of the Delaney laboratory for helpful discussion.

ABBREVIATIONS

5-caC, 5-carboxycytosine; 5-fC, 5-formylcytosine; 5-FU, 5-fluorouracil; 5-mC, 5-methylcytosine; AcCoA, acetyl coenzyme A; AcK, acetyl-lysine; ANOVA, analysis of variance; AP, apurinic/apyrimidinic; APE1, AP endonuclease 1; BER, base excision repair; C, cytosine; DDR, DNA damage response; G, guanine, glycine; IDP/R, intrinsically disordered proteins/regions; K, lysine; K_D, dissociation constant; k_{max}, maximal single turnover rate; k_{STO}, observed single turnover rate; k_{TO}, turnover rate; LLPS, liquid-liquid phase separation; MBD4, methyl binding domain 4; MTO, multiple turnover; NAD^+/NADH, nicotinamide adenine dinucleotide; PAGE, polyacrylamide gel electrophoresis; PCNA,

proliferating cell nuclear antigen; polβ, DNA polymerase β; PTM, post-translational modification; Q, glutamine; S, serine; STO, single turnover; T, thymine; TS, thymidylate synthase; TDG, thymine DNA glycosylase; U, uracil; Y, tyrosine

ACCESSION CODES

H. sapiens TDG, Uniprot entry Q13569

REFERENCES

(1) Baugh, E. H.; Ke, H.; Levine, A. J.; Bonneau, R. A.; Chan, C. S. Why are there hotspot mutations in the TP53 gene in human cancers? *Cell Death Differ.* **2018**, *25* (1), 154-160.
(2) Gold, B. Somatic mutations in cancer: Stochastic versus predictable. *Mutat. Res. Genet. Toxicol. Environ. Mutagen.* **2017**, *814*, 37-46.
(3) Devarakonda, S.; Rotolo, F.; Tsao, M.-S.; Lanc, I.; Brambilla, E.; Masood, A.; Olaussen, K. A.; Fulton, R.; Sakashita, S.; McLeer-Florin, A. Tumor mutation burden as a biomarker in resected non–small-cell lung cancer. *J. Clin. Oncol.* **2018**, *36* (30), 2995.
(4) Schermerhorn, K. M.; Delaney, S. A Chemical and Kinetic Perspective on Base Excision Repair of DNA. *Acc. Chem. Res.* **2014**, *47* (4), 1238-1246.
(5) Brooks, S. C.; Adhikary, S.; Rubinson, E. H.; Eichman, B. F. Recent advances in the structural mechanisms of DNA glycosylases. *Biochim Biophys Acta Proteins Proteom* **2013**, *1834* (1), 247-271.
(6) Aravind, L.; Koonin, E. V. The α/β fold uracil DNA glycosylases: a common origin with diverse fates. *Genome Biol* **2000**, *1* (4), research0007.0001.
(7) Wiebauer, K.; Jiricny, J. In vitro correction of G o T mispairs to G o C pairs in nuclear extracts from human cells. *Nature* **1989**, *339*, 234.
(8) Neddermann, P.; Jiricny, J. Efficient removal of uracil from GU mispairs by the mismatch-specific thymine DNA glycosylase from HeLa cells. *Proc. Natl. Acad. Sci. U.S.A.* **1994**, *91* (5), 1642-1646.
(9) Gallinari, P.; Jiricny, J. A new class of uracil-DNA glycosylases related to human thymine-DNA glycosylase. *Nature* **1996**, *383* (6602), 735.
(10) Bennett, M. T.; Rodgers, M.; Hebert, A. S.; Ruslander, L. E.; Eisele, L.; Drohat, A. C. Specificity of human thymine DNA glycosylase depends on N-glycosidic bond stability. *J. Am. Chem. Soc.* **2006**, *128* (38), 12510-12519.
(11) Morgan, M. T.; Bennett, M. T.; Drohat, A. C. Excision of 5-Halogenated Uracils by Human Thymine DNA Glycosylase Robust Activity for DNA Contexts other than CpG. *J. Biol. Chem.* **2007**, *282* (38), 27578-27586.
(12) Maiti, A.; Morgan, M. T.; Pozharski, E.; Drohat, A. C. Crystal structure of human thymine DNA glycosylase bound to DNA elucidates sequence-specific mismatch recognition. *Proc. Natl. Acad. Sci. U.S.A.* **2008**, *105* (26), 8890-8895.
(13) Coey, C. T.; Malik, S. S.; Pidugu, L. S.; Varney, K. M.; Pozharski, E.; Drohat, A. C. Structural basis of damage recognition by thymine DNA glycosylase: Key roles for N-terminal residues. *Nucleic Acids Res.* **2016**, *44* (21), 10248-10258.

(14) Kohli, R. M.; Zhang, Y. TET enzymes, TDG and the dynamics of DNA demethylation. *Nature* **2013**, *502* (7472), 472-479.
(15) He, Y.-F.; Li, B.-Z.; Li, Z.; Liu, P.; Wang, Y.; Tang, Q.; Ding, J.; Jia, Y.; Chen, Z.; Li, L. Tet-mediated formation of 5-carboxylcytosine and its excision by TDG in mammalian DNA. *Science* **2011**, *333* (6047), 1303-1307.
(16) Zhang, L.; Lu, X.; Lu, J.; Liang, H.; Dai, Q.; Xu, G.-L.; Luo, C.; Jiang, H.; He, C. Thymine DNA glycosylase specifically recognizes 5-carboxylcytosine-modified DNA. *Nat. Chem. Biol.* **2012**, *8* (4), 328-330.
(17) Neddermann, P.; Gallinari, P.; Lettieri, T.; Schmid, D.; Truong, O.; Hsuan, J. J.; Wiebauer, K.; Jiricny, J. Cloning and expression of human G/T mismatch-specific thymine-DNA glycosylase. *J. Biol. Chem.* **1996**, *271* (22), 12767-12774.
(18) Baba, D.; Maita, N.; Jee, J.-G.; Uchimura, Y.; Saitoh, H.; Sugasawa, K.; Hanaoka, F.; Tochio, H.; Hiroaki, H.; Shirakawa, M. Crystal structure of thymine DNA glycosylase conjugated to SUMO-1. *Nature* **2005**, *435* (7044), 979-982.
(19) Baba, D.; Maita, N.; Jee, J.-G.; Uchimura, Y.; Saitoh, H.; Sugasawa, K.; Hanaoka, F.; Tochio, H.; Hiroaki, H.; Shirakawa, M. Crystal structure of SUMO-3-modified thymine-DNA glycosylase. *J. Mol. Biol.* **2006**, *359* (1), 137-147.
(20) Smet-Nocca, C.; Wieruszeski, J.-M.; Chaar, V.; Leroy, A.; Benecke, A. The Thymine−DNA Glycosylase Regulatory Domain: Residual Structure and DNA Binding. *Biochemistry* **2008**, *47* (25), 6519-6530.
(21) Cortázar, D.; Kunz, C.; Saito, Y.; Steinacher, R.; Schär, P. The enigmatic thymine DNA glycosylase. *DNA Repair (Amst.)* **2007**, *6* (4), 489-504.
(22) Abu, M.; Waters, T. R. The main role of human thymine-DNA glycosylase is removal of thymine produced by deamination of 5-methylcytosine and not removal of ethenocytosine. *J. Biol. Chem.* **2003**, *278* (10), 8739-8744.
(23) Hang, B.; Medina, M.; Fraenkel-Conrat, H.; Singer, B. A 55-kDa protein isolated from human cells shows DNA glycosylase activity toward 3, N4-ethenocytosine and the G/T mismatch. *Proc. Natl. Acad. Sci. U.S.A.* **1998**, *95* (23), 13561-13566.
(24) Saparbaev, M.; Laval, J. 3, N4-ethenocytosine, a highly mutagenic adduct, is a primary substrate for Escherichia coli double-stranded uracil-DNA glycosylase and human mismatch-specific thymine-DNA glycosylase. *Proc. Natl. Acad. Sci. U.S.A.* **1998**, *95* (15), 8508-8513.
(25) Dow, B. J.; Malik, S. S.; Drohat, A. C. Defining the role of nucleotide flipping in enzyme specificity using 19F NMR. *J. Am. Chem. Soc.* **2019**, *141* (12), 4952-4962.
(26) Fitzgerald, M. E.; Drohat, A. C. Coordinating the Initial Steps of Base Excision Repair: Apurinic/Apyrimidinc Endonuclease I Actively Stimulates Thymine DNA Glycosylase by Disrupting the Product Complex. *J. Biol. Chem.* **2008**, *283* (47), 32680-32690.
(27) Waters, T. R.; Gallinari, P.; Jiricny, J.; Swann, P. F. Human thymine DNA glycosylase binds to apurinic sites in DNA but is displaced by human apurinic endonuclease 1. *J. Biol. Chem.***1999**, *274* (1), 67-74.
(28) Cortázar, D.; Kunz, C.; Selfridge, J.; Lettieri, T.; Saito, Y.; MacDougall, E.; Wirz, A.; Schuermann, D.; Jacobs, A. L.; Siegrist, F.; Steinacher, R.; Jiricny, J.; Bird, A.; Schär, P. Embryonic lethal phenotype reveals a function of TDG in maintaining epigenetic stability. *Nature* **2011**, *470* (7334), 419.

(29) DeNizio, J. E.; Dow, B. J.; Serrano, J. C.; Ghanty, U.; Drohat, A. C.; Kohli, R. M. TET-TDG Active DNA Demethylation at CpG and Non-CpG Sites. *J. Mol. Biol.* **2021**, *433* (8), 166877.
(30) Shimizu, Y.; Iwai, S.; Hanaoka, F.; Sugasawa, K. Xeroderma pigmentosum group C protein interacts physically and functionally with thymine DNA glycosylase. *EMBO J* **2003**, *22* (1), 164-173.
(31) Madabushi, A.; Hwang, B.-J.; Jin, J.; Lu, A.-L. Histone deacetylase SIRT1 modulates and deacetylates DNA base excision repair enzyme thymine DNA glycosylase. *Biochem* **2013**, *456* (1), 89-98.
(32) Guan, X.; Madabushi, A.; Chang, D.-Y.; Fitzgerald, M. E.; Shi, G.; Drohat, A. C.; Lu, A.-L. The human checkpoint sensor Rad9–Rad1–Hus1 interacts with and stimulates DNA repair enzyme TDG glycosylase. *Nucleic Acids Res.* **2007**, *35* (18), 6207-6218.
(33) Dancy, B. M.; Cole, P. A. Protein lysine acetylation by p300/CBP. *Chem. Rev.* **2015**, *115* (6), 2419-2452.
(34) Chen, D.; Lucey, M. J.; Phoenix, F.; Lopez-Garcia, J.; Hart, S. M.; Losson, R.; Buluwela, L.; Coombes, R. C.; Chambon, P.; Schär, P. T: G mismatch-specific thymine-DNA glycosylase potentiates transcription of estrogen-regulated genes through direct interaction with estrogen receptor α. *J. Biol. Chem.* **2003**, *278* (40), 38586-38592.
(35) Shibata, E.; Dar, A.; Dutta, A. CRL4Cdt2 E3 ubiquitin ligase and proliferating cell nuclear antigen (PCNA) cooperate to degrade thymine DNA glycosylase in S phase. *J. Biol. Chem.* **2014**, *289* (33), 23056-23064.
(36) Tini, M.; Benecke, A.; Um, S.-J.; Torchia, J.; Evans, R. M.; Chambon, P. Association of CBP/p300 acetylase and thymine DNA glycosylase links DNA repair and transcription. *Mol. Cell* **2002**, *9* (2), 265-277.
(37) Henry, R. A.; Mancuso, P.; Kuo, Y.-M.; Tricarico, R.; Tini, M.; Cole, P. A.; Bellacosa, A.; Andrews, A. J. Interaction with the DNA Repair Protein Thymine DNA Glycosylase Regulates Histone Acetylation by p300. *Biochemistry* **2016**, *55* (49), 6766-6775.
(38) Lucey, M. J.; Chen, D.; Lopez-Garcia, J.; Hart, S. M.; Phoenix, F.; Al-Jehani, R.; Alao, J. P.; White, R.; Kindle, K. B.; Losson, R. T: G mismatch-specific thymine-DNA glycosylase (TDG) as a coregulator of transcription interacts with SRC1 family members through a novel tyrosine repeat motif. *Nucleic Acids Res.* **2005**, *33* (19), 6393-6404.
(39) Li, Y.-Q.; Zhou, P.-Z.; Zheng, X.-D.; Walsh, C. P.; Xu, G.-L. Association of Dnmt3a and thymine DNA glycosylase links DNA methylation with base-excision repair. *Nucleic Acids Res.* **2006**, *35* (2), 390-400.
(40) Slenn, T. J.; Morris, B.; Havens, C. G.; Freeman, R. M.; Takahashi, T. S.; Walter, J. C. Thymine DNA glycosylase is a CRL4Cdt2 substrate. *J. Biol. Chem.* **2014**, *289* (33), 23043-23055.
(41) Steinacher, R.; Schär, P. Functionality of human thymine DNA glycosylase requires SUMO-regulated changes in protein conformation. *Curr. Biol.* **2005**, *15* (7), 616-623.
(42) Mohan, R. D.; Rao, A.; Gagliardi, J.; Tini, M. SUMO-1-dependent allosteric regulation of thymine DNA glycosylase alters subnuclear localization and CBP/p300 recruitment. *Mol. Cell. Biol.* **2007**, *27* (1), 229-243.
(43) McLaughlin, D.; Coey, C. T.; Yang, W.-C.; Drohat, A. C.; Matunis, M. J. Characterizing requirements for small ubiquitin-like modifier (SUMO) modification and

binding on base excision repair activity of thymine-DNA glycosylase in vivo. *J. Biol. Chem.* **2016**, *291* (17), 9014-9024.
(44) Coey, C. T.; Drohat, A. C. Defining the impact of sumoylation on substrate binding and catalysis by thymine DNA glycosylase. *Nucleic Acids Res.* **2018**, *46* (10), 5159-5170.
(45) Hardeland, U.; Steinacher, R.; Jiricny, J.; Schär, P. Modification of the human thymine-DNA glycosylase by ubiquitin-like proteins facilitates enzymatic turnover. *EMBO J* **2002**, *21* (6), 1456-1464.
(46) Mohan, R. D.; Litchfield, D. W.; Torchia, J.; Tini, M. Opposing regulatory roles of phosphorylation and acetylation in DNA mispair processing by thymine DNA glycosylase. *Nucleic Acids Res.* **2009**, *38* (4), 1135-1148.
(47) Thompson, P. R.; Kurooka, H.; Nakatani, Y.; Cole, P. A. Transcriptional Coactivator Protein p300. *J. Biol. Chem.* **2001**, *276* (36), 33721-33729.
(48) Liu, T.; Liu, P. Y.; Marshall, G. M. The critical role of the class III histone deacetylase SIRT1 in cancer. *Cancer Res.* **2009**, *69* (5), 1702-1705.
(49) Kabra, N.; Li, Z.; Chen, L.; Li, B.; Zhang, X.; Wang, C.; Yeatman, T.; Coppola, D.; Chen, J. SirT1 is an inhibitor of proliferation and tumor formation in colon cancer. *J. Biol. Chem.* **2009**, *284* (27), 18210-18217.
(50) Kolthur-Seetharam, U.; Dantzer, F.; McBurney, M. W.; de Murcia, G.; Sassone-Corsi, P. Control of AIF-mediated Cell Death by the Functional Interplay of SIRT1 and PARP-1 in Response to DNA Damage. *Cell Cycle* **2006**, *5* (8), 873-877.
(51) Solomon, J. M.; Pasupuleti, R.; Xu, L.; McDonagh, T.; Curtis, R.; DiStefano, P. S.; Huber, L. J. Inhibition of SIRT1 Catalytic Activity Increases p53 Acetylation but Does Not Alter Cell Survival following DNA Damage. *Mol. Cell. Biol.* **2006**, *26* (1), 28-38.
(52) Rajamohan, S. B.; Pillai, V. B.; Gupta, M.; Sundaresan, N. R.; Birokov, K. G.; Samant, S.; Hottiger, M. O.; Gupta, M. P. SIRT1 Promotes Cell Survival under Stress by Deacetylation-Dependent Deactivation of Poly(ADP-Ribose) Polymerase 1. *Mol. Cell. Biol.* **2009**, *29* (15), 4116-4129.
(53) Yamamoto, H.; Schoonjans, K.; Auwerx, J. Sirtuin Functions in Health and Disease. *Mol. Endocrinol.* **2007**, *21* (8), 1745-1755.
(54) Yamamori, T.; DeRicco, J.; Naqvi, A.; Hoffman, T. A.; Mattagajasingh, I.; Kasuno, K.; Jung, S.-B.; Kim, C.-S.; Irani, K. SIRT1 deacetylates APE1 and regulates cellular base excision repair. *Nucleic Acids Res.* **2010**, *38* (3), 832-845.
(55) Hasan, S.; Stucki, M.; Hassa, P. O.; Imhof, R.; Gehrig, P.; Hunziker, P.; Hübscher, U.; Hottiger, M. O. Regulation of Human Flap Endonuclease-1 Activity by Acetylation through the Transcriptional Coactivator p300. *Mol. Cell* **2001**, *7*, 1221-1231.
(56) Hasan, S.; El-Andaloussi, N.; Hardeland, U.; Hassa, P. O.; Bürki, C.; Imhof, R.; Schär, P.; Hottiger, M. O. Acetylation Regulates the DNA End-Trimming Activity of the DNA Polymerase Beta. *Mol. Cell* **2002**, *10*, 1213-1222.
(57) Katsyuba, E.; Romani, M.; Hofer, D.; Auwerx, J. NAD+ homeostasis in health and disease. *Nature Metab.* **2020**, *2* (1), 9-31.
(58) Kunz, C.; Focke, F.; Saito, Y.; Schuermann, D.; Lettieri, T.; Selfridge, J.; Schär, P. Base excision by thymine DNA glycosylase mediates DNA-directed cytotoxicity of 5-fluorouracil. *PLoS Biol.* **2009**, *7* (4), e1000091.
(59) Longley, D. B.; Harkin, D. P.; Johnston, P. G. 5-fluorouracil: mechanisms of action and clinical strategies. *Nat. Rev. Cancer* **2003**, *3* (5), 330-338.

(60) Derissen, E. J.; Jacobs, B. A.; Huitema, A. D.; Rosing, H.; Schellens, J. H.; Beijnen, J. H. Exploring the intracellular pharmacokinetics of the 5-fluorouracil nucleotides during capecitabine treatment. *Br. J. Clin. Pharmacol.* **2016**, *81* (5), 949-957.
(61) Park, J. H.; Zhao, M.; Han, Q.; Sun, Y.; Higuchi, T.; Sugisawa, N.; Yamamoto, J.; Singh, S. R.; Clary, B.; Bouvet, M. Efficacy of oral recombinant methioninase combined with oxaliplatinum and 5-fluorouracil on primary colon cancer in a patient-derived orthotopic xenograft mouse model. *Biochem. Biophys. Res. Commun.* **2019**, *518* (2), 306-310.
(62) Xie, P.; Mo, J.-L.; Liu, J.-H.; Li, X.; Tan, L.-M.; Zhang, W.; Zhou, H.-H.; Liu, Z.-Q. Pharmacogenomics of 5-fluorouracil in colorectal cancer: review and update. *Cell Oncol (Dordr)* **2020**, *43*, 989-1001.
(63) Fang, L.; Jiang, Y.; Yang, Y.; Zheng, Y.; Zheng, J.; Jiang, H.; Zhang, S.; Lin, L.; Zheng, J.; Zhang, S. Determining the optimal 5-FU therapeutic dosage in the treatment of colorectal cancer patients. *Oncotarget* **2016**, *7* (49), 81880.
(64) Christenson, E. S.; Gizzi, A.; Cui, J.; Egleston, M.; Seamon, K. J.; DePasquale, J.; Orris, B.; Park, B. H.; Stivers, J. T. Inhibition of Human Uracil DNA Glycosylase Sensitizes a Large Fraction of Colorectal Cancer Cells to 5-Fluorodeoxyuridine and Raltitrexed but Not Fluorouracil. *Mol Pharmacol* **2021**, *99*, 412-425.
(65) Team, R. C. R: A language and environment for statistical computing. R Foundation for Statistical Computing, Vienna, Austria 2017.
(66) Choudhary, C.; Kumar, C.; Gnad, F.; Nielsen, M. L.; Rehman, M.; Walther, T. C.; Olsen, J. V.; Mann, M. Lysine Acetylation Targets Protein Complexes and Co-Regulates Major Cellular Functions. *Science* **2009**, *325* (5942), 834.
(67) Kamieniarz, K.; Schneider, R. Tools to Tackle Protein Acetylation. *Chem. Biol.* **2009**, *16* (10), 1027-1029.
(68) Waters, T. R.; Swann, P. F. Kinetics of the action of thymine DNA glycosylase. *J. Biol. Chem.* **1998**, *273* (32), 20007-20014.
(69) Wolfe, A. E.; O'Brien, P. J. Kinetic mechanism for the flipping and excision of 1, N 6-ethenoadenine by human alkyladenine DNA glycosylase. *Biochemistry* **2009**, *48* (48), 11357-11369.
(70) Sassa, A.; Beard, W. A.; Shock, D. D.; Wilson, S. H. Steady-state, Pre-steady-state, and Single-turnover Kinetic Measurement for DNA Glycosylase Activity. *JoVE* **2013**, (78), e50695.
(71) Johnson, K. A.; Goody, R. S. The original Michaelis constant: translation of the 1913 Michaelis–Menten paper. *Biochemistry* **2011**, *50* (39), 8264-8269.
(72) Maiti, A.; Drohat, A. C. Dependence of substrate binding and catalysis on pH, ionic strength, and temperature for thymine DNA glycosylase: Insights into recognition and processing of G·T mispairs. *DNA Repair (Amst.)* **2011**, *10* (5), 545-553.
(73) Dodd, T.; Yan, C.; Kossmann, B. R.; Martin, K.; Ivanov, I. Uncovering universal rules governing the selectivity of the archetypal DNA glycosylase TDG. *Proc. Natl. Acad. Sci. U.S.A.* **2018**, *115* (23), 5974-5979.
(74) Da, L.-T.; Yu, J. Base-flipping dynamics from an intrahelical to an extrahelical state exerted by thymine DNA glycosylase during DNA repair process. *Nucleic Acids Res.* **2018**, *46* (11), 5410-5425.
(75) Drohat, A. C.; Maiti, A. Mechanisms for enzymatic cleavage of the N-glycosidic bond in DNA. *Org. Biomol. Chem.* **2014**, *12* (42), 8367-8378.

(76) Morgan, M. T.; Maiti, A.; Fitzgerald, M. E.; Drohat, A. C. Stoichiometry and affinity for thymine DNA glycosylase binding to specific and nonspecific DNA. *Nucleic Acids Res.* **2011**, *39* (6), 2319-2329.
(77) Bhakat, K. K.; Hazra, T. K.; Mitra, S. Acetylation of the human DNA glycosylase NEIL2 and inhibition of its activity. *Nucleic Acids Res.* **2004**, *32* (10), 3033-3039.
(78) Weinert, B. T.; Narita, T.; Satpathy, S.; Srinivasan, B.; Hansen, B. K.; Schölz, C.; Hamilton, W. B.; Zucconi, B. E.; Wang, W. W.; Liu, W. R.; Brickman, J. M.; Kesicki, E. A.; Lai, A.; Bromberg, K. D.; Cole, P. A.; Choudhary, C. Time-Resolved Analysis Reveals Rapid Dynamics and Broad Scope of the CBP/p300 Acetylome. *Cell* **2018**, *174* (1), 231-244.e212.
(79) Albaugh, B. N.; Arnold, K. M.; Denu, J. M. KAT (ching) metabolism by the tail: insight into the links between lysine acetyltransferases and metabolism. *Chembiochem* **2011**, *12* (2), 290.
(80) Hubbard, B. P.; Gomes, A. P.; Dai, H.; Li, J.; Case, A. W.; Considine, T.; Riera, T. V.; Lee, J. E.; E, S. Y.; Lamming, D. W.; Pentelute, B. L.; Schuman, E. R.; Stevens, L. A.; Ling, A. J. Y.; Armour, S. M.; Michan, S.; Zhao, H.; Jiang, Y.; Sweitzer, S. M.; Blum, C. A.; Disch, J. S.; Ng, P. Y.; Howitz, K. T.; Rolo, A. P.; Hamuro, Y.; Moss, J.; Perni, R. B.; Ellis, J. L.; Vlasuk, G. P.; Sinclair, D. A. Evidence for a Common Mechanism of SIRT1 Regulation by Allosteric Activators. *Science* **2013**, *339* (6124), 1216-1219.
(81) Wang, F.; Marshall, C. B.; Ikura, M. Transcriptional/epigenetic regulator CBP/p300 in tumorigenesis: structural and functional versatility in target recognition. *Cell. Mol. Life Sci.* **2013**, *70* (21), 3989-4008.
(82) Lavau, C.; Du, C.; Thirman, M.; Zeleznik-Le, N. Chromatin-related properties of CBP fused to MLL generate a myelodysplastic-like syndrome that evolves into myeloid leukemia. *EMBO J* **2000**, *19* (17), 4655-4664.
(83) Gervais, C.; Murati, A.; Helias, C.; Struski, S.; Eischen, A.; Lippert, E.; Tigaud, I.; Penther, D.; Bastard, C.; Mugneret, F. Acute myeloid leukaemia with 8p11 (MYST3) rearrangement: an integrated cytologic, cytogenetic and molecular study by the groupe francophone de cytogenetique hematologique. *Leukemia* **2008**, *22* (8), 1567-1575.
(84) van der Lee, R.; Buljan, M.; Lang, B.; Weatheritt, R. J.; Daughdrill, G. W.; Dunker, A. K.; Fuxreiter, M.; Gough, J.; Gsponer, J.; Jones, D. T.; Kim, P. M.; Kriwacki, R. W.; Oldfield, C. J.; Pappu, R. V.; Tompa, P.; Uversky, V. N.; Wright, P. E.; Babu, M. M. Classification of Intrinsically Disordered Regions and Proteins. *Chem. Rev.* **2014**, *114* (13), 6589-6631.
(85) Habchi, J.; Tompa, P.; Longhi, S.; Uversky, V. N. Introducing Protein Intrinsic Disorder. *Chem. Rev.* **2014**, *114* (13), 6561-6588.
(86) Larson, A. G.; Elnatan, D.; Keenen, M. M.; Trnka, M. J.; Johnston, J. B.; Burlingame, A. L.; Agard, D. A.; Redding, S.; Narlikar, G. J. Liquid droplet formation by HP1α suggests a role for phase separation in heterochromatin. *Nature* **2017**, *547* (7662), 236-240.
(87) Turner, A. L.; Watson, M.; Wilkins, O. G.; Cato, L.; Travers, A.; Thomas, J. O.; Stott, K. Highly disordered histone H1− DNA model complexes and their condensates. *Proc. Natl. Acad. Sci. U.S.A.* **2018**, *115* (47), 11964-11969.
(88) Deckard III, C. E.; Sczepanski, J. T. Reversible chromatin condensation by the DNA repair and demethylation factor thymine DNA glycosylase. *Nucleic Acids Res.* **2021**, *49* (5), 2450-2459.

(89) Bhakat, K. K.; Mokkapati, S. K.; Boldogh, I.; Hazra, T. K.; Mitra, S. Acetylation of human 8-oxoguanine-DNA glycosylase by p300 and its role in 8-oxoguanine repair in vivo. *Mol. Cell. Biol.* **2006**, *26* (5), 1654-1665.
(90) Izawa, S.; Inoue, Y.; Kimura, A. Oxidative stress response in yeast: effect of glutathione on adaptation to hydrogen peroxide stress in Saccharomyces cerevisiae. *FEBS Lett.* **1995**, *368* (1), 73-76.
(91) Haigis, M. C.; Sinclair, D. A. Mammalian sirtuins: biological insights and disease relevance. *Ann Rev Pathol* **2010**, *5*, 253-295.
(92) Strom, A. R.; Emelyanov, A. V.; Mir, M.; Fyodorov, D. V.; Darzacq, X.; Karpen, G. H. Phase separation drives heterochromatin domain formation. *Nature* **2017**, *547* (7662), 241-245.

For Table of Contents use only